

UNCLASSIFIED

AD

405 900

DEFENSE DOCUMENTATION CENTER

FOR

SCIENTIFIC AND TECHNICAL INFORMATION

CAMERON STATION, ALEXANDRIA, VIRGINIA



UNCLASSIFIED

NOTICE: When government or other drawings, specifications or other data are used for any purpose other than in connection with a definitely related government procurement operation, the U. S. Government thereby incurs no responsibility, nor any obligation whatsoever; and the fact that the Government may have formulated, furnished, or in any way supplied the said drawings, specifications, or other data is not to be regarded by implication or otherwise as in any manner licensing the holder or any other person or corporation, or conveying any rights or permission to manufacture, use or sell any patented invention that may in any way be related thereto.

SSD-TDR-63-106

63-3-6

①

REPORT NO.  
TDR-169(3101)

*Grade 1*

405900

AD No. \_\_\_\_\_

FILE COPY

# Feasibility Study of the Control of the Mercury/Atlas Booster Re-Entry from Orbital Missions

15 MAY 1963

*Prepared by*

D. PACE and T. SHIOKARI

*Prepared for* COMMANDER SPACE SYSTEMS DIVISION

UNITED STATES AIR FORCE

*Inglewood, California*

405 900

DDC  
RECEIVED  
JUN 11 1963  
TISIA A

ENGINEERING DIVISION • AEROSPACE CORPORAT  
CONTRACT NO. AF 04(695)

*5*

④ 5.60

⑤ 17505

SSD-TDR-63-106

⑭ Report No.  
TDR 169(3101)TN/1  
≠ ≠ ≠ ≠

⑥

FEASIBILITY STUDY OF THE  
CONTROL OF THE MERCURY/ATLAS  
BOOSTER RE-ENTRY FROM ORBITAL MISSIONS,

⑦-⑧-⑨ NA

⑩ Prepared by  
D. Pace and T. Shiokari  
Engineering Division

⑫ 54p.

AEROSPACE CORPORATION  
El Segundo, California

C

⑬ NA

⑭ ⑮ ⑯ +

⑰ NA

⑰ Contract No. AF 04(695)-169  
≠ ≠

⑱ U

⑲ NA

⑪ 15 May 1963

FD

Prepared for  
COMMANDER SPACE SYSTEMS DIVISION  
UNITED STATES AIR FORCE  
Inglewood, California

C

SSD-TDR-63-106

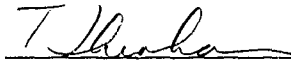
Report No.  
TDR-169(3101)TN-1

FEASIBILITY STUDY OF THE  
CONTROL OF THE MERCURY/ATLAS  
BOOSTER RE-ENTRY FROM ORBITAL MISSIONS

Prepared by:

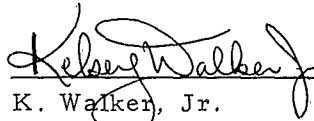


D. Pace  
Systems Department

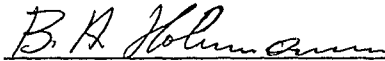


T. Shiokari  
Mercury Launch Vehicle Program Office

Approved by:



K. Walker, Jr.  
Head, Systems Department  
Spacecraft Engineering Subdivision



B. A. Hohmann  
Systems Engineering Director  
NASA Manned Launch Vehicle Programs

AEROSPACE CORPORATION  
El Segundo, California

ABSTRACT

An investigation was undertaken into the feasibility of deorbiting the Mercury/Atlas booster in such a way as to prevent fragments of the booster from falling on land masses and to do this without compromising Mercury mission objectives. This report summarizes the various methods explored and presents the conclusions thereof.

---

CONTENTS

ABSTRACT . . . . .	iii
I INTRODUCTION . . . . .	1
II RECOVERY HISTORY . . . . .	1
III RE-ENTRY TRAJECTORIES AND DISPERSION . . . . .	3
IV ATLAS DEORBIT CAPABILITY . . . . .	5
V DISCUSSION . . . . .	11
VI CONCLUSIONS . . . . .	13
VII REFERENCES . . . . .	15
VIII TABLES AND FIGURES . . . . .	17

## I. INTRODUCTION

Fragments from the Mercury/Atlas orbital missions have been recovered in foreign countries. These fragments have been thoroughly analyzed by the manufacturer of the booster and most of the fragments were identified as parts from the Mercury/Atlas final booster stage. Apprehension involving the possibility of problems in international relations arising from the impact of these fragments on foreign soil, prompted the Air Force to request a feasibility study to determine if the impacting fragments could be controlled without jeopardizing the present Mercury Program.

There have been instances where identifying markings on the fragments recovered established the missile serial number and the physical location of the parts on the missile airframe. The number of orbits was then established by impact location and time of observation and from orbit calculations with the impact area longitude and latitude as a set of end conditions. The results of these studies are summarized in this report.

The report is primarily a feasibility study as to the basic characteristics necessary to deorbit the final stage of the launch vehicle. No attempt is made to determine when or how the launch vehicle is destroyed during the re-entry phase. Such an attempt to determine the mechanics of breakup would require a detailed re-entry analysis and is not in the scope of this investigation. A brief discussion is, however, presented concerning the problems associated with the deliberate destruction of the airframe into fragments of such size as to be consumed during the re-entry heating.

## II. RECOVERY HISTORY

The recovery of fragments from Mercury/Atlas sustainers has been officially reported after two of the five orbital missions, i. e., MA-6 and MA-8. The

chronological order of launches, number of fragments recovered, and the number of passes are shown on Table I. The spacecraft injection conditions were identical for these two missions except for the inertial velocity which was increased 20 fps for Mission MA-8. These injection requirements were met within injection tolerance limits on all missions.

Following orbit injection, the spacecraft separation sequence imparts a relative velocity increment between the booster and spacecraft from the spacecraft postgrade engines. The net effect on velocity differential between the spacecraft and sustainer has been an average of 28 fps which consists of 6 fps Atlas sustainer velocity decrease and 22 fps spacecraft velocity increase.

The first reported recovery was from MA-6, where a total of 12 fragments were reported. An extensive study was conducted to identify and determine the physical condition of the fragments and their position on the booster. The results of this study (References 1, 2 and 3) are summarized in Table II and Figure 2. A later study indicates that the South American parts have not been positively identified as fragments from MA-6 booster.

Assuming the fragments were from MA-6, the distance between the two reported areas of recovery would amount to approximately 4400 N.M. The parts recovered were fragments from the lox and fuel tank. However, the South African recovery had a higher percentage from the lox tank and the South American recovery had a higher percentage from the fuel tank.

The spectographic analysis on the selected surfaces indicated that the South African parts encountered higher re-entry heating (1600°F to 2000°F for short duration) than the pieces from South America which showed evidence of severe aerodynamic heating only along the edges (Reference 2). From calculations of the heat transfer and physical damage, the sphere recovered in South Africa appears to have re-entered the heating period in a shielded condition (Reference 3).

### III. RE-ENTRY TRAJECTORIES AND DISPERSIONS

To determine the feasibility of deorbiting the sustainer shortly after spacecraft separation, a brief study was made of nominal impact points as a function of ballistic coefficient, retro-fire angle and retro-velocity. Preliminary efforts were directed toward establishing the effect of retro-velocity on range from the point of deboost. A ballistic coefficient ( $W/C_D A$ ) of  $5.5 \text{ lb/ft}^2$  corresponding approximately to a tumbling, intact sustainer stage, and retro-velocities ranging from 100 to 1000 ft/sec were assumed in this analysis. Figure 3 shows the points of impact for several of these retro-velocities at a retro-fire angle of 150 degrees (clockwise) from the local horizontal. Figures 4 and 5 show impact latitude and longitude as a function of retro-fire angle and velocity. The 100 ft/sec deboost velocity resulted in no deorbit.

It was clear from this analysis, which is given in more detail later in this report, that a deboost system capable of insuring impact west of the continental limits of Africa would be excessively heavy and would seriously jeopardize the primary Mercury mission. Attention was therefore directed to retro-velocities in the region between 100 and 200 ft/sec to determine the feasibility of impacting in the Indian Ocean. The study was to include ballistic coefficients of 2.25, 5.5 and  $11.0 \text{ lb/ft}^2$ . In addition, a limited dispersion analysis was made to determine the effects of injection errors on impact. For purposes of this study, three sigma errors of  $\pm 0.2$  degrees in injection, flight path angle and  $\pm 20$  ft/sec in injection velocity were assumed. The retro-fire angles were from 140 to 170 degrees (clockwise) with respect to the local horizontal, and retro-velocities were from 140 to 180 ft/sec.

All trajectory calculations were made on the IBM 7090 using a three degree of freedom trajectory program, which includes a rotating, oblate earth and

the 1959 ARDC Standard Atmosphere. Initial conditions prior to deboost were obtained from Reference 4 and are as follows:

Velocity (Inertial)	25,710 ft/sec.
Altitude	528,420 ft
Flight Path Angle (Inertial)	90 deg.
Azimuth Heading (Inertial)	77.53 deg. East of North
Longitude	72.43 deg. West
Latitude (Geodetic)	30 15 deg. North

Deboost was simulated by providing thrust at a level of 1710 pounds. The velocity increment added was determined by the time of thrust. The value of 1710 pounds was chosen only for computational convenience. For all trajectories, re-entry was assumed to begin at an altitude of 400,000 feet.

Tables III through V give the impact latitude, longitude and range, from the point of deboost for the nominal cases. Tables VI through XVII show similar results for the dispersed trajectories. Figures 6 through 14 show the differential ranges between the nominal impact points and the dispersed impact points. For geographical orientation, Figure 15 shows the debris impact line for ballistic coefficients between 2.25 and 11.0 lb/ft<sup>2</sup>, with flight path angle deviations of ±0.2 degree, and retro-velocity of 160 ft/sec. The latter value was selected because it is approximately the minimum velocity which insures impact in the presence of dispersions for the range of ballistic coefficients used in this study. It is emphasized that the impact line indicated is for the three sigma injection flight path errors and does not include injection velocity errors. To obtain the total three sigma dispersions, the range errors from flight angle and the range errors from velocity must be root-sum-squared. For instance, at a retro-velocity of 160 ft/sec., retro-fire angle of 160 degrees and a ballistic coefficient of 11.0 lbs/ft<sup>2</sup>, the three sigma range error about the nominal impact line is:

$$\Delta R = \begin{matrix} +2850 \text{ N.M.} \\ -2050 \text{ N.M.} \end{matrix}$$

$$\text{Nominal Range} = 7170 \text{ N.M.}$$

C

As can be seen, the three sigma maximum range from point of deboost is over 10,000 miles. For the very small re-entry angles encountered for the deboost, the prediction of a range of this magnitude is subject to the same vagaries as orbit lifetime predictions. Indeed, it is not inconceivable that atmospheric variations with respect to the ARDC Standard would result in significant increases in range or even no deorbit at all on that pass. Furthermore, for values of ballistic coefficient around  $2.25 \text{ lb/ft}^2$  and for a retro-velocity of 160 ft/sec, the nominal impact point is in South Africa. Since this value of ballistic coefficient is close to that of a tank fragment, there is no reason to assume that re-entering pieces would be burned up before impact.

C

It is evident therefore, that attempting to deboost with retro-velocities on the order of 150 ft/sec cannot guarantee impact outside of the populated land masses, and under certain circumstances, cannot even guarantee successful deorbit. It should be noted that an inherent assumption in this conclusion is that vehicle breakup occurs at a sufficiently high altitude so that the ballistic coefficient has a significant effect on the impact line. Although not directly comparable, the observed dispersion of MA-6 and MA-8 lends some weight to this assumption.

Consideration was given to the possibility of delaying deboost until the impact lines were east of Africa. However, such a delay would require the addition of an attitude control system and possible major revision to the Atlas autopilot with corresponding weight increase and possible reduction in reliability. For this reason, no detailed analyses were made and the approach abandoned.

#### IV. ATLAS DEORBIT CAPABILITY

##### A. ATLAS ATTITUDE FOLLOWING SECO:

C

The Atlas attitude following SECO is random due to angle-of-attack dispersion at spacecraft separation and due to its tumbling motion following separation.

The angle-of-attack (angle between acceleration vector and velocity vector) dispersion has been determined analytically by performing trajectory calculations with various missile non-standard flight conditions.

The result of this study is shown in Table XVIII where the nominal angle-of-attack is  $-4.8^\circ$  and the 1 sigma RSS value is  $\begin{matrix} +2.3^\circ \\ -3.2^\circ \end{matrix}$ . The flight angles-of-attack from tracking data of the Mercury orbital missions are as follows:

MA-5	$-4.4^\circ$
MA-6	$-3.0^\circ$
MA-7	$0.1^\circ$

NOTE: Negative sign is pitch down.

The above table illustrates that the flight results investigated are within the analytically derived dispersion.

In addition to the angle-of-attack, a small angle exists between the acceleration vector and missile centerline due to center-of-gravity offset. This angle can be established prior to launch with reasonable accuracy. The nominal value for Mercury is  $0.7^\circ$ .

The tumbling motion of the missile following spacecraft separation is obtainable from the telemetered gyro data. This data is shown on Figures 16 through 18 for all orbital flights from SECO to SECO + 20 seconds and is derived from integrating the rate gyro data. The randomness of the tumbling motion is depicted on these graphs. For the T + 4 seconds data slice, the following missile tumbling attitudes are obtained:

	<u>Pitch</u>	<u>Yaw</u>	<u>Roll</u>
MA-4	$2.15^\circ$	$0.40^\circ$	$0.40^\circ$
MA-5	$-0.7^\circ$	$-6.40^\circ$	$-3.60^\circ$
MA-6	$-2.6^\circ$	$-2.50^\circ$	$-1.80^\circ$
MA-7	$2.8^\circ$	$2.0^\circ$	$1.0^\circ$
MA-8	$-3.0^\circ$	$-1.5^\circ$	$-1.7^\circ$

From this sample of data, the arithmetic mean and standard deviation are:

Mean	-0.27	-1.6	-1.15
1σ	2.7°	3.2°	1.9°

The resulting missile pitch attitude dispersion from the effects of angle-of-attack dispersions and tumbling motion is:

$$1\sigma_{RSS} = \sqrt{(3.2)^2 + (2.7)^2} = 4.2$$

or a three sigma deviation of 12.6°

The above T + 4 seconds for the time slice was determined from examining the time of spacecraft posigrade initiation. These times are:

Time from SECO to:

	<u>0.2g's</u>	<u>Posigrade Fire</u>
MA-4	0.94 sec.	2.15 sec.
MA-5	0.71	1.77
MA-6	0.93	2.10
MA-7	0.52	1.59
MA-8	<u>1.06</u>	<u>1.96</u>
Arithmetic Mean	0.832	1.914

The standard deviations of the above set are:

1σ	0.215	0.233
----	-------	-------

From these values, the three sigma maximum is 2.61 seconds for capsule separation from SECO. The T + 4.0 seconds is therefore a conservative value to use to insure complete capsule separation.

## B. ATLAS RETRO-ROCKETS

The Atlas has retro-rockets for separating the booster from the weapon system payloads. These rocket characteristics are presented in Table XIX and are designated as Marc 7A and Marc 8A. The Marc 7A is mounted as a cluster of two in the B-2 pod at station 874. The thrust vector is 14 degrees from the missile centerline. Marc 8A is mounted 6 inches forward of each vernier engine and parallel to the missile centerline.

## C. RETRO-CAPABILITY ABOARD ATLAS

Other sources of retro-impulse aboard the Atlas that can be made available are the vernier engines and the lox tank gasses. The weight penalty from these sources is small, since a major portion of the hardware or energy source is presently aboard; however, they would require some modification to the subsystems that are affected.

Use of the impulse that is available from the pressurized gasses (gox and helium) in the lox tank by bursting the lox tank access hole was considered. With this diaphragm ruptured from the access hole, an orifice of approximately 200 in<sup>2</sup> is available. The analysis (Reference 6) then considered two extreme gas mixture conditions: (1) gox and helium remaining stratified and (2) gox and helium mixed. The resulting impulse computed for the first case (stratified gas) was approximately 8160 lb/sec and for the second case (uniform mixture) was approximately 13,400 lb/sec. The impulse time would be approximately 9.6 sec to drop the tank pressure to 1 psia and the initial thrust would be approximately 6,000 lb.

The present vernier engine gimbaling capability is +20° to -30° (inward) in the yaw plane about a nominal 30 degrees from missile centerline. The gimbaling in the pitch plane is limited to ±70°. In order to have more travel, the engine gearing and the vehicle actuator would have to be modified. A feasibility study shows that the vernier engines could be designed for extended gimbal excursion, allowing use of the verniers as a retro-rocket (Reference 9).

The start tanks (propellants for vernier engine solo), in addition to modifying the vernier engines, would have to be refilled as in the weapon system. The present Mercury boosters have no vernier solo phase. Refilling the start tanks would penalize the Mercury performance by 111 lb of lox and fuel. For the existing Mercury configuration, the start tanks are partially filled to 81 lb of lox and 69 lb of fuel. The resulting total vernier propellant available would then be 261 lb (Reference 8).

The vernier engine characteristics are as follows (Reference 7):

	<u>Altitude</u>
Thrust, Lb.	984
Specific Impulse, Sec	235.4
Total Impulse, Lb. Sec	22,200
Minimum Guaranteed Burn Time, Sec	22.5

A second problem associated with the verniers, is the necessity for vernier restart capability. The existing SECO command is a shutdown of both the vernier and sustainer engines. This shutdown sequence of the vernier engines could be eliminated at SECO by initiating the gimbaling of the verniers to impart a reverse thrust and the effect on the payload would be minimal since the present spacecraft separation sequence is initiated when the longitudinal g's decay to 0.2 g's; but, during this sequence of events, and during the duration of vernier solo reversed thrust, the autopilot would be required to operate for missile stability and for programming the events.

The feasibility study on vernier gimbaling also indicated that the engine performance can be increased and the hardware weight reduced. It was estimated that engine characteristics would improve by 20 percent (Reference 9). The improvement is achieved by increasing the expansion ratio.

#### D. RETRO-CAPABILITY AND REQUIREMENT

For the determination of the velocity increment that could be imparted by the impulse sources discussed, the thrust vector is assumed to be directed

through the missile center of gravity and the missile is stable during the thrust period. With the vernier engines in operation, adequate control and stability should be available during the transition and impulse duration. Also, the velocity increment assumes a 7,500 lb. mass to be decelerated. With this large vehicle mass and the relatively small effective propellant mass being considered (low vehicle mass ratio) the velocity increment calculation is approximated, based on the following simplified relationship:

$$\Delta V = \frac{\text{total impulse}}{\text{total vehicle mass}}$$

The resulting velocity increments for the various impulse sources are:

<u>Impulse Source</u>	<u>Duration (sec)</u>	<u>Total Impulse lb. sec.</u>	<u>Ratio Velocity Increment(fps)</u>
1. Pod Installation (2-Marc 7A)	1.0	960	4
2. Vernier Mount (2-Marc 8A)	1.5	2,440	11
3. Lox Tank Gas	9.6	10,800	46
4. Vernier Engines (Present System)	22.5	44,400	190
5. Vernier Engines (Improved Version)	45.0	54,000	232

#### E. PLANNED FRAGMENTIZATION OF BOOSTER

Planned fragmentization of the booster to ensure that the fragments would be consumed during re-entry heating, appears to be the simplest hardware implementation method.

This can be accomplished by a destruct system, which would fragmentize the sustainer engine hardware and initiate tank explosion. However, several problems are associated with this technique. The major technical problems are to assure that the fragment size and the ballistic coefficients are in

proper relationship for the parts to be consumed during re-entry, and that the velocity imparted will be relatively low in order to minimize the effect of dispersion.

The time set for the initiation of the booster destruct, such as during orbit or re-entry phase, will introduce additional problems. If the destruct is initiated during orbit, a timing sequence can be utilized but a destruct in orbit will cause some fragments to go into higher energy orbits and remain orbiting for some time, with a probability of hitting the spacecraft.

If the destruct is to be accomplished during re-entry, the time of destruct initiation is a problem because present knowledge of atmospheric density is not well enough established to predict decay orbit re-entry with any accuracy. Other means such as command destruct and onboard self-logic g's or temperature control may be feasible. The command destruct method would require a multitude of ground command stations because of the earth's curvature. The self-logic method would have the major problem of engineering satisfactory reliability for safety during powered flight and for operation during re-entry. Also, the determination of re-entry environment would be difficult to establish since the missile orientation and tumbling motion will be random.

## V. DISCUSSION

With the present Mercury spacecraft insertion characteristics, the analysis indicates that the Atlas launch vehicle has a very limited region for impacting outside of the land mass area. For the area west of Africa (Atlantic Ocean), the minimum retro-velocity increment is 600 fps. With reasonable development effort and still maintaining the Mercury performance capability, the maximum the Atlas is capable of retro-ing is 276 fps. This velocity would result in a nominal impact on Africa. The minimum retro-velocity which will insure impact considering the dispersions, is 160 fps, which still results in a nominal impact on the eastern portion of Africa.

Any possible utilization of this low velocity increment would require that the retro-fire time be delayed a sufficient length of time so that the nominal impact will be east of Africa. The duration of this delay is approximately 15 minutes, and for that length of time the vehicle would require a continued attitude control because of its inherent tumbling motion. The vernier engines have the controlability but not the duration of impulse time.

In addition, the study indicates that the impact dispersion increases with decrease in retro-velocity. The dispersion at the low retro-velocity results primarily from retro-velocity variations, flight path angle variations and the possible spread in the ballistic coefficient.

Missile perturbations such as missile drifting following SECO and the variation in missile centerline with the flight path at SECO, appear to have relatively small effect on re-entry trajectory dispersions if the retro-fire angle is properly selected. To illustrate this argument, the following comparison is made, assuming the retro-velocity increment is 160 fps, retro-fire angle of  $\alpha = 170^\circ$ , and  $W/C_D A = 11.0 \text{ lb/ft}^2$ .

<u>Error Source</u>	<u>Dispersion</u>	
For $\alpha = 170^\circ$		
( $\Delta V$ error of 20 fps)	+1780 N. M.	- 930 N.M.
( $\Delta V$ error of $0.2^\circ$ )	+1710	-1780
	<hr/>	<hr/>
3 $\sigma$ RSS	+2470	-2010
For $\alpha = 170^\circ + 13^\circ = 183^\circ$		
( $\Delta V$ error of 20 fps)	+2120	- 950
( $\Delta V$ error of $0.2^\circ$ )	+2220	-1860
	<hr/>	<hr/>
3 $\sigma$ RSS	+3070	-2090

The 13 degree angular dispersion in the retro-fire angle changes the impact dispersion by  $-80 + 600 \text{ N.M.}$ . Considering the other dispersions, this effect is relatively small.

## VI. CONCLUSIONS

- A. A low (near minimum) retro-velocity increment will not result in impact of the Atlas sustainer outside of land mass area if retro-fire is initiated subsequent to SECO.
- B. A high (greater than 600 fps) retro-velocity increment will insure impact in the Atlantic Ocean; however, this cannot be attained with developed hardware or by modifying available hardware. To have the capability of imparting this velocity, the weight penalty will be prohibitive for the Mercury mission since the external impulse source must be carried by the booster throughout the powered flight phase.
- C. Fragmenting the Atlas sustainer by an explosive device is too unreliable for assurance that fragments will be destroyed during re-entry.
- D. Implementation of any controlled re-entry device of the Atlas sustainer is not feasible within the present scope of Mercury Mission.

## VII. REFERENCES

1. "Investigation of Recovered Fragments from Atlas 109D Booster"; GD/A Report No. AE 62-0558; J. J. Sheppard Jr.; 1 July 1962.
2. "Investigation of Atlas Fragments Recovered in Brazil"; GD/A Report No. AE 62-0797; M. Sibulkin and W. H. Gallaher; 20 August 1962.
3. "Investigation of Recovered Fragments from Atlas 109D Booster - Supplemental Information"; GD/A Report No. AE 62-0828; W. H. Gallaher; 14 Sept. 1962.
4. Unpublished Trajectory Listing; "Milestone for Bill Brocato, Case MA-9, Case 1, Run 8"; 21 November 1962.
5. IOC, "Review of Non-Standard Flight Conditions for Simulation"; AS 1933.21-843; T. Shiokari; 28 November 1962.
6. IOC, "Impulse Available from Gas in Lox Tank at SECO"; AS 1933.21-36; R. G. Olander; 14 January 1963.
7. "Design Information Report for the MA-5 Propulsion System"; Rocketdyne Report No. R-3026-1; 15 August 1962.
8. IOC, "Atlas Mass Properties for Mercury Terminal Conditions"; AS 63-1943.2-3; J. W. Newbold; 7 January 1963.
9. "Atlas MA-5 Improved Engine System for Space Applications"; Rocketdyne, R-2830P; 3 January 1961.

Table I. Mercury/Atlas Recovery History

<u>Launch Date</u>	<u>Mission Number</u>	<u>Booster Number</u>	<u>No. of Parts</u>	<u>Location of Recovery</u>	<u>Booster Injection Velocity (FPS)</u>	<u>Re-entry (No. of Orbits)</u>
13 Sept 1961	MA-4	88D	0	--	25,675	--
29 Nov 1961	MA-5	93D	0	--	25,679	--
20 Feb 1962	MA-6	109D	{ <sup>6</sup> * 6	So. Africa So. America	25,702	6
24 May 1962	MA-7	107D	0	--	25,711	--
3 Oct 1962	MA-8	113D	3	No. West Africa	25,724	16 or 42**

\* The So. American parts are not positively identified as parts from MA-6.

\*\* Orbit calculation being conducted by GD/A to determine the number of passes.

Table II. MA-6 (109D) General Fragment Data

<u>No.</u>	<u>Mat'l</u>	<u>Size (in.)</u>	<u>Area (ft<sup>2</sup>)</u>	<u>Weight (lbs)</u>	<u>Recovered Location</u>
1	301 SS	38 X 45 X (.014 and .015)	8.8	6.9	30°28'S X 26°49'E
2	301 SS	40 X 45 X (.014 and .015)	8.2	5.9	30°28'S X 26°49'E
3	301 SS	8 X 160 X (.044)	9.8	12.3	30°28'S X 26°49'E
4	Titanium	21 dia. (.018) Sphere	2.4	47.8	30°28'S X 26°49'E
5	301 SS Ti-phenolic	46 X 50 (.010 and .016)	12.3	20.5	30°58'S X 27°36'E
6	301 SS	20 X 25 X (.020)	3.1	2.0	31°46'S X 18°37'E
7	301 SS	24 X 23 X (.016 and .018)	2.7	2.0	21°05'S X 43°25'W
8	301 SS	15 X 18 X (.028)	1.5	2.0	21°05'S X 43°25'W
9	301 SS	13 X 4 X (.024)	0.3	0.25	21°05'S X 43°25'W
10	301 SS	24 X 41 X (.028)	5.2	6.25	21°05'S X 43°25'W
11	301 SS	26 X 56 X (.0154 and .016)	12.1	9.0	21°05'S X 43°25'W
12	301 SS	29 X 29 X (.022)	4.4	6.25	19°30'S X 46°31'W

Note: Refer to Figure 2 for physical location on the missile.

Table III. Impact, Latitude, Longitude, and Range for Nominal Deboost

$$\underline{W/C_D A = 2.25 \text{ lb/ft}^2}$$

Retrovelocity = 150 fps

<u>Retrofire Angle, Deg</u>	<u>Impact Latitude, Deg</u>	<u>Impact Longitude, Deg</u>	<u>Impact Range, N M</u>
140	7.22 N	23.85 E	5485
150	8.03 N	22.62 E	5398
160	7.24 N	23.80 E	5482
170	5.08 N	26.99 E	5711

Retrovelocity = 160 fps

140	10.93 N	18.14 E	5081
150	11.29 N	17.57 E	5042
160	10.34 N	19.06 E	5146
170	8.21 N	22.33 E	5377

Retrovelocity = 180 fps

140	16.19 N	9.41 E	4483
150	16.05 N	9.64 E	4498
160	14.96 N	11.53 E	4625
170	12.92 N	14.94 E	4859

Table IV. Impact Latitude, Longitude, and Range for Nominal Deboost  
 $W/C_D A = 5.5 \text{ lb/ft}^2$

Retrovelocity = 150 fps

<u>Retrofire Angle, Deg</u>	<u>Impact Latitude, Deg</u>	<u>Impact Longitude, Deg</u>	<u>Impact Range, N M</u>
140	21.07 S	68.77 E	8621
150	13.38 S	54.62 E	7691
160	11.60 S	51.72 E	7491
170	12.98 S	53.94 E	7645

Retrovelocity = 160 fps

140	10.35 S	49.77 E	7354
150	5.93 S	43.04 E	6876
160	5.30 S	42.11 E	6809
170	7.07 S	44.73 E	6965

Retrovelocity = 180 fps

140	2.00 N	31.51 E	6039
150	3.69 N	29.05 E	5860
160	3.29 N	29.63 E	5902
170	1.25 N	32.57 E	6116

Table V. Impact Latitude, Longitude, and Range for Nominal Deboost

$$\underline{W/C_D A = 11.0 \text{ lb/ft}^2}$$

Retrovelocity = 150 fps

<u>Retrofire Angle, Deg</u>	<u>Impact Latitude, Deg</u>	<u>Impact Longitude, Deg</u>	<u>Impact Range, N M</u>
140	29.32 S	91.57 E	9943
150	18.78 S	64.17 E	8328
160	15.80 S	58.72 E	7969
170	16.66 S	60.24 E	8131

Retrovelocity = 160 fps

140	16.36 S	59.72 E	8096
150	10.03 S	49.26 E	7279
160	8.70 S	47.20 E	7173
170	10.16 S	49.44 E	7332

Retrovelocity = 180 fps

140	1.50 S	36.59 E	6408
150	.91 N	33.09 E	6154
160	.82 N	33.22 E	6163
170	1.08 S	35.96 E	6363

Table VI. Impact Latitude, Longitude, and Range for Dispersed Deboost  
Flight Path Angle Dispersion = +0.2 Deg

$W/C_D A = 2.25 \text{ lb/ft}^2$

Retrovelocity = 150 fps

<u>Retrofire Angle, Deg</u>	<u>Impact Latitude, Deg</u>	<u>Impact Longitude, Deg</u>	<u>Impact Range, N M</u>
140	12.55 S	53.23 E	7596
150	7.48 S	45.33 E	7041
160	6.28 S	43.52 E	6911
170	7.38 S	45.17 E	7029

Retrovelocity = 160 fps

140	5.30 S	42.09 E	6808
150	1.95 S	37.20 E	6454
160	1.50 S	36.54 E	6406
170	2.96 S	38.64 E	6559

Retrovelocity = 180 fps

140	4.64 N	27.65 E	5759
150	6.10 N	25.50 E	5604
170	3.88 N	28.73 E	5838

Table VII. Impact Latitude, Longitude, and Range for Dispersed Deboost

Flight Path Angle Dispersion = +0.2 Deg

$W/C_D A = 5.5 \text{ lb/ft}^2$

Retrovelocity = 150 fps

<u>Retrofire Angle, Deg</u>	<u>Impact Latitude, Deg</u>	<u>Impact Longitude, Deg</u>	<u>Impact Range, N M</u>
140	No Deorbit		
150	32.60 S	114.84 E	11185
160	29.00 S	90.26 E	9872
170	27.44 S	84.82 E	9571

Retrofire velocity = 160 fps

140	No Deorbit		
150	27.01 S	83.50 E	9498
160	22.49 S	71.79 E	8809
170	21.70 S	70.06 E	8702

Retrofire velocity = 180 fps

140	20.29 S	67.14 E	8518
150	13.11 S	54.15 E	7660
160	10.96 S	50.69 E	7420
170	11.58 S	51.65 E	7487

Table VIII. Impact Latitude, Longitude, and Range for Dispersed Deboost

Flight Angle Dispersion = +0.2 Deg

$W/C_D A = 11.0 \text{ lb/ft}^2$

Retrovelocity = 150 fps

<u>Retrofire Angle, Deg</u>	<u>Impact Latitude, Deg</u>	<u>Impact Longitude, Deg</u>	<u>Impact Range, N M</u>
140	No Deorbit		
150	32.44 S	126.26 E	11747
160	31.26 S	101.03 E	10432
170	29.61 S	92.68 E	10003

Retrovelocity = 160 fps

140	No Deorbit		
150	30.21 S	95.39 E	10145
160	25.40 S	78.89 E	9233
170	24.17 S	75.74 E	9047

Retrovelocity = 180 fps

140	24.76 S	77.26 E	9137
150	16.30 S	59.58 E	8087
160	13.55 S	54.87 E	7709
170	13.84 S	55.34 E	7741

Table IX. Impact Latitude, Longitude, and Range for Dispersed Deboost  
Flight Path Angle Dispersion = -0.2 Deg  
 $W/C_D A = 2.25 \text{ lb/ft}^2$

Retrovelocity = 150 fps

<u>Retrofire Angle, Deg</u>	<u>Impact Latitude, Deg</u>	<u>Impact Longitude, Deg</u>	<u>Impact Range, N M</u>
140	19.28 N	3.68 E	4107
150	18.89 N	4.43 E	4156
160	17.78 N	6.53 E	4292
170	15.87 N	9.97 E	4520

Retrovelocity = 160 fps

140	20.91 N	0.39 E	3898
150	20.47 N	1.31 E	3956
160	19.38 N	3.48 E	4094
170	17.56 N	6.92 E	4318

Retrovelocity = 180 fps

140	23.40 N	5.09 W	3559
150	22.90 N	3.94 W	3629
160	21.86 N	1.64 W	3771
170	20.21 N	1.82 E	3988

Table X. Impact Latitude, Longitude, and Range for Dispersed Deboost

Flight Path Angle Dispersion = -0.2 Deg

$$\underline{W/C_D A = 5.5 \text{ lb/ft}^2}$$

Retrovelocity = 150 fps

<u>Retrofire Angle, Deg</u>	<u>Impact Latitude, Deg</u>	<u>Impact Longitude, Deg</u>	<u>Impact Range, N M</u>
140	8.52 N	21.89 E	5345
150	8.95 N	21.23 E	5298
160	7.96 N	22.83 E	5417
170	5.62 N	26.22 E	5656

Retrovelocity = 160 fps

140	11.77 N	16.82 E	4988
150	11.90 N	16.62 E	4975
160	10.85 N	18.28 E	5090
170	8.63 N	21.70 E	5332

Retrovelocity = 180 fps

140	16.38 N	9.08 E	4461
150	16.17 N	9.44 E	4485
160	15.09 N	11.33 E	4612
170	13.08 N	14.69 E	4841

Table XI. Impact Latitude, Longitude, and Range for Dispersed Deboost

Flight Path Angle Dispersion = -0.2 Deg

$W/C_D A = 11.0 \text{ lb/ft}^2$

Retrovelocity = 150 fps

<u>Retrofire Angle, Deg</u>	<u>Impact Latitude, Deg</u>	<u>Impact Longitude, Deg</u>	<u>Impact Range, N M</u>
140	5.04 N	27.10 E	5719
150	5.96 N	25.73 E	5620
160	5.15 N	26.93 E	5707
170	2.79 N	30.37 E	5956

Retrovelocity = 160 fps

140	8.94 N	21.25 E	5300
150	9.39 N	20.55 E	5250
160	8.46 N	21.98 E	5351
170	6.22 N	25.34 E	5558

Retrovelocity = 180 fps

140	14.31 N	12.67 E	4702
150	14.27 N	12.72 E	4706
160	13.24 N	14.44 E	4823
170	11.19 N	17.73 E	5052

Table XII. Impact Latitude, Longitude, and Range for Dispersed Deboost

Velocity Magnitude Dispersion = + 20ft/sec

$W/C_D A = 2.25 \text{ lb/ft}^2$

Retrovelocity = 150 fps

<u>Retrofire Angle, Deg</u>	<u>Impact Latitude, Deg</u>	<u>Impact Longitude, Deg</u>	<u>Impact Range, N M</u>
140	0.88 S	35.68 E	6334
150	1.46 N	32.29 E	6095
160	1.05 N	32.88 E	6141
170	1.37 S	36.36 E	6392

Retrovelocity = 160 fps

140	5.21 N	26.83 E	5699
150	6.38 N	25.08 E	5573
160	5.57 N	26.28 E	5660
170	3.14 N	29.84 E	5918

Retrovelocity = 180 fps

140	12.87 N	15.04 E	4865
150	13.01 N	14.80 E	4849
160	11.87 N	16.64 E	4976
170	9.53 N	20.31 E	5234

Table XIII. Impact, Latitude, Longitude, and Range for Dispersed Deboost

Velocity Magnitude Dispersion = +20 ft/sec

$W/C_D A = 5.5 \text{ lb/ft}^2$

Retrovelocity = 150 fps

<u>Retrofire Angle, Deg</u>	<u>Impact Latitude, Deg</u>	<u>Impact Longitude, Deg</u>	<u>Impact Range, N M</u>
140	No Deorbit		
150	No Deorbit		
160	30.67 S	97.71 E	10265
170	29.82 S	93.64 E	10053

Retrovelocity = 160 fps

140	No Deorbit		
150	23.58 S	74.35 E	8964
160	19.35 S	65.26 E	8399
170	20.18 S	66.91 E	8504

Retrovelocity = 180 fps

140	9.73 S	48.79 E	7286
150	4.98 S	41.64 E	6775
160	4.48 S	40.90 E	6772
170	6.57 S	43.98 E	6944

Table XIV. Impact Latitude, Longitude, and Range for Dispersed Deboost

Velocity Magnitude Dispersion = + 20 ft/sec

$$\underline{W/C_D A = 11.0 \text{ lb/ft}^2}$$

Retrovelocity = 150 fps

<u>Retrofire Angle, Deg</u>	<u>Impact Latitude, Deg</u>	<u>Impact Longitude, Deg</u>	<u>Impact Range, N M</u>
140	No Deorbit		
150	No Deorbit		
160	No Deorbit		
170	No Deorbit		

Retrovelocity = 160 fps

140	No Deorbit		
150	30.69 S	97.82 E	10271
160	24.82 S	77.43 E	9147
170	24.62 S	76.90 E	9116

Retrovelocity = 180 fps

140	16.27 S	59.57 E	8086
150	9.20 S	47.98 E	7228
160	7.91 S	46.01 E	7088
170	9.67 S	48.68 E	7278

Table XV. Impact Latitude, Longitude, and Range for Dispersed Deboost

Velocity Magnitude Dispersion = -20 ft/sec

$W/C_D A = 2.25 \text{ lb/ft}^2$

Retrovelocity = 150 fps

<u>Retrofire Angle, Deg</u>	<u>Impact Latitude, Deg</u>	<u>Impact Longitude Deg</u>	<u>Impact Range N M</u>
140	12.10 N	16.28 E	4951
150	12.33 N	15.90 E	4925
160	11.46 N	17.29 E	5021
170	9.57 N	20.25 E	5711

Retrovelocity = 160 fps

140	14.70 N	11.99 E	4657
150	14.70 N	11.97 E	4655
160	13.75 N	13.56 E	4764
170	11.89 N	16.60 E	4973

Retrovelocity = 180 fps

140	18.60 N	4.98 E	4192
150	18.34 N	5.48 E	4225
160	17.31 N	7.37 E	4348
170	15.52 N	10.55 E	4560

Table XVI. Impact, Latitude, Longitude, and Range for Dispersed Deboost  
Velocity Magnitude Dispersion = -20 ft/sec  
 $W/C_D A = 5.5 \text{ lb/ft}^2$

Retrovelocity = 150 fps

<u>Retrofire Angle, Deg</u>	<u>Impact Latitude, Deg</u>	<u>Impact Longitude, Deg</u>	<u>Impact Range, N M</u>
140	3.88 S	40.04 E	6659
150	1.34 S	36.34 E	6391
160	1.24 S	36.19 E	6380
170	2.91 S	38.60 E	6555

Retrovelocity = 160 fps

140	1.23 N	32.62 E	6119
150	2.88 N	30.23 E	5946
160	2.61 N	30.61 E	5974
170	0.85 N	33.16 E	6159

Retrovelocity = 180 fps

140	8.38 N	22.09 E	5360
150	9.05 N	21.06 E	5287
160	8.38 N	22.08 E	5360
170	6.54 N	24.84 E	5562

Table XVII. Impact Latitude, Longitude and Range for Dispersed Deboost  
Velocity Magnitude Dispersion = -20 ft/sec  
 $W/C_D A = 11.0 \text{ lb/ft}^2$

Retrovelocity = 150 fps

<u>Retrofire Angle, Deg</u>	<u>Impact Latitude, Deg</u>	<u>Impact Longitude, Deg</u>	<u>Impact Range N M</u>
140	8.05 S	46.22 E	7105
150	4.58 S	41.05 E	6733
160	4.07 S	40.30 E	6678
170	5.55 S	42.47 E	6835

Retrovelocity = 160 fps

140	2.13 S	37.49 E	6474
150	0.14 N	34.20 E	6235
160	0.16 N	34.17 E	6232
170	1.48 S	36.53 E	6404

Retrovelocity = 180 fps

140	5.92 N	25.77 E	5623
150	6.93 N	24.27 E	5515
160	6.42 N	25.02 E	5569
170	4.64 N	27.64 E	5758

Table XVIII.  $\beta$  Angle Dispersion from Flight Simulation\*

$\beta$  = Angle between acceleration vector and velocity vector.

	<u><math>3\sigma</math></u>		<u><math>\Delta</math></u>	
	High	Low	(Nominal = $-4.8^\circ$ )	
Thrust (Booster and Sustainer)	$-2.6^\circ$	$-7.0^\circ$	2.2	-2.2
Autopilot Pitch Program (Attenuated - gain)	$+1.7^\circ$	$-14.2^\circ$	6.5	-9.4
Gyro Drift (Nose-up - Nose-down)	$-3.6^\circ$	$-6.0^\circ$	1.2	-1.2
Weight Dispersions	$-4.3^\circ$	$-5.3^\circ$	.5	-.5
		$3\sigma$ RSS	<u>7.0<sup>o</sup></u>	<u>-9.8<sup>o</sup></u>

\*STL - Unpublished trajectory simulation listings, R Evans,  
21 March 1963.

Table XIX. Characteristics of Atlas Retro Rockets

<u>Nomenclature</u>	<u>Marc 7A</u>	<u>Marc 8A</u>
Thrust at 70°F (Vacuum) lb	440	860
Burn time, sec	1.04	1.48
Total Impulse at 70°F (Vacuum) lb sec	480	1220
Weight, lb	5.25	17.7
Diameter, in	2.9	5.5
Overall Length	14.7	16.75
Expansion Ratio	25.6	18

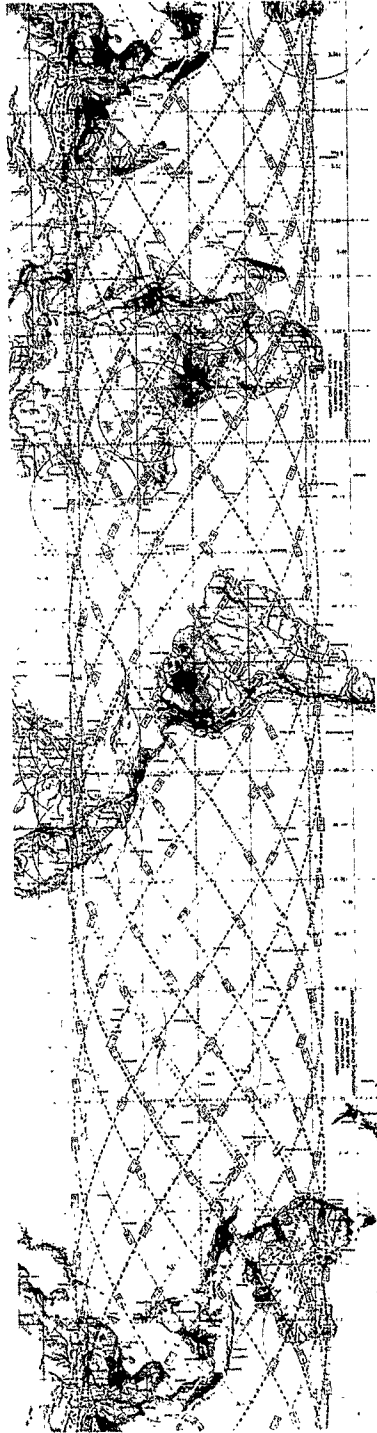


Figure 1. Mercury Spacecraft Orbit Chart.

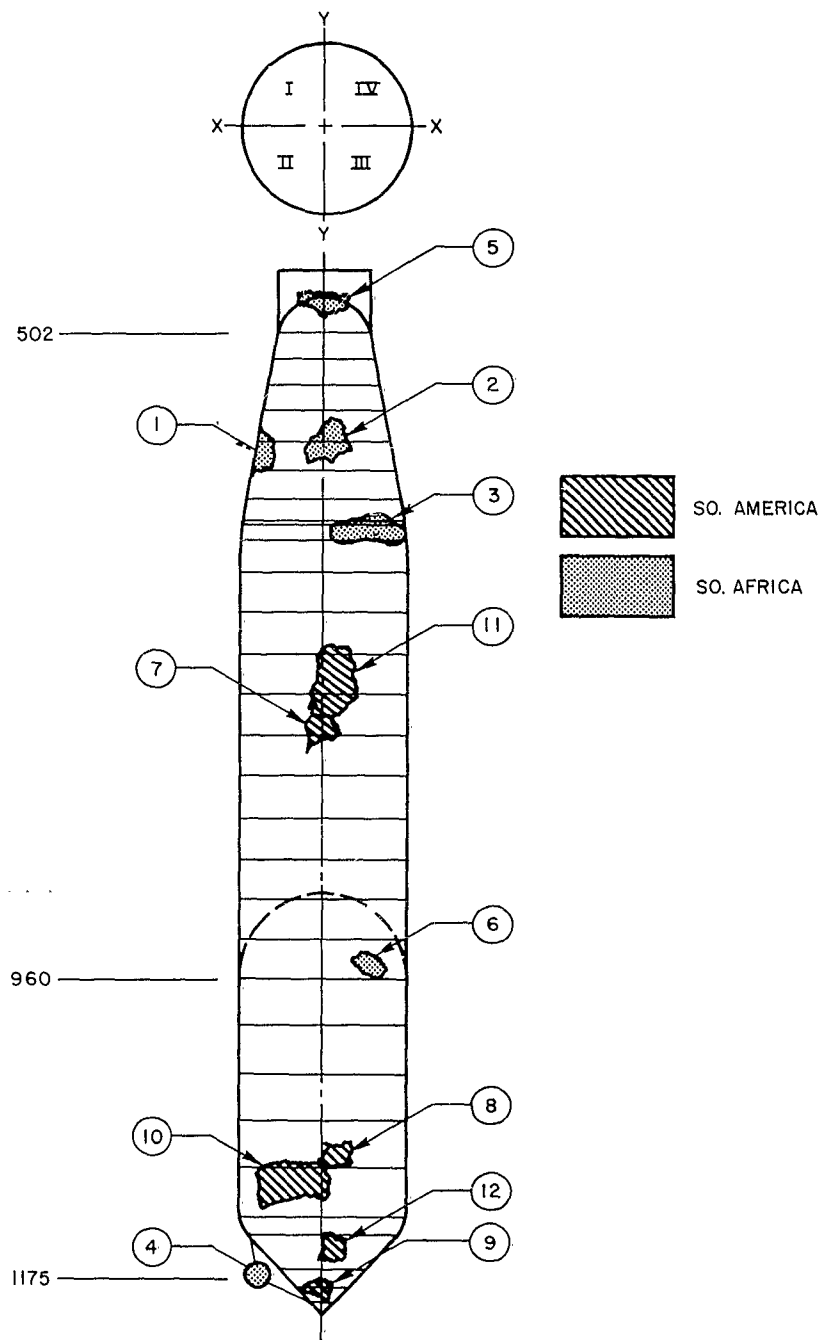


Figure 2. MA-6 Fragment Location on Missile.

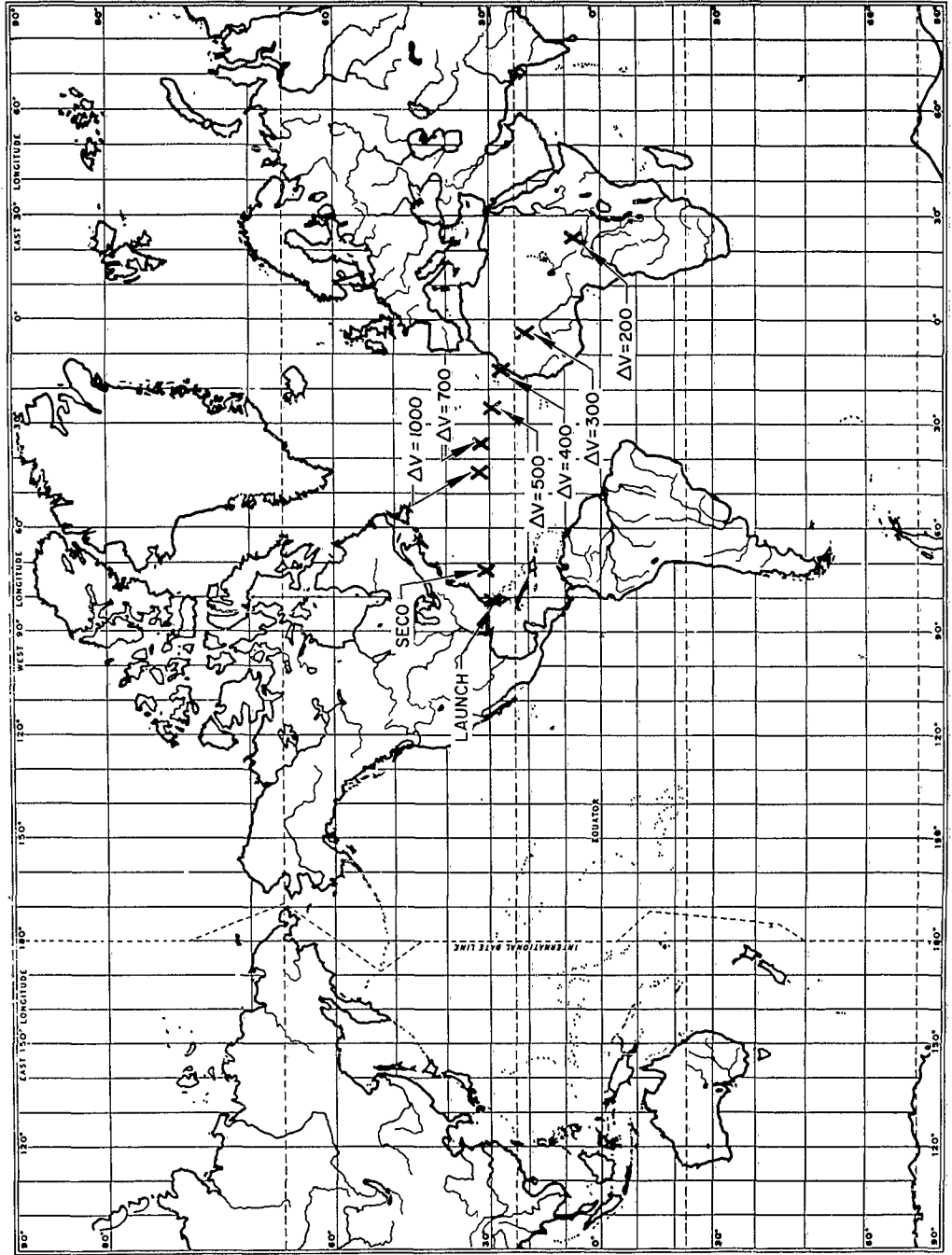


Figure 3. Nominal Impact as a Function of Retro-Velocity  
 $W/C_D A = 5.5 \text{ lb/ft}^2$  and Retro-Angle =  $150^\circ$ .

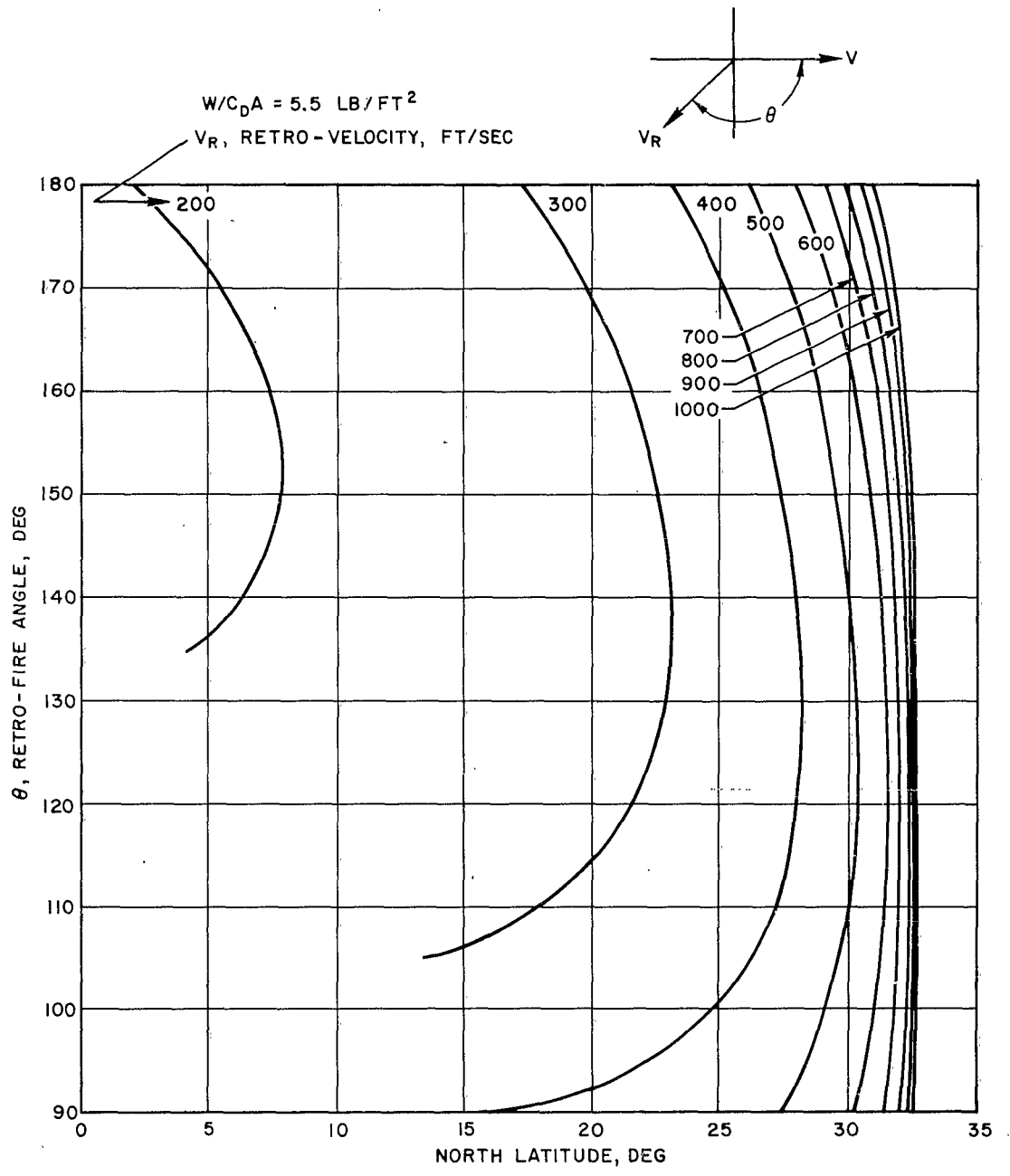


Figure 4. Impact Latitude as a Function of Retro-fire Angle and Retro-velocity.

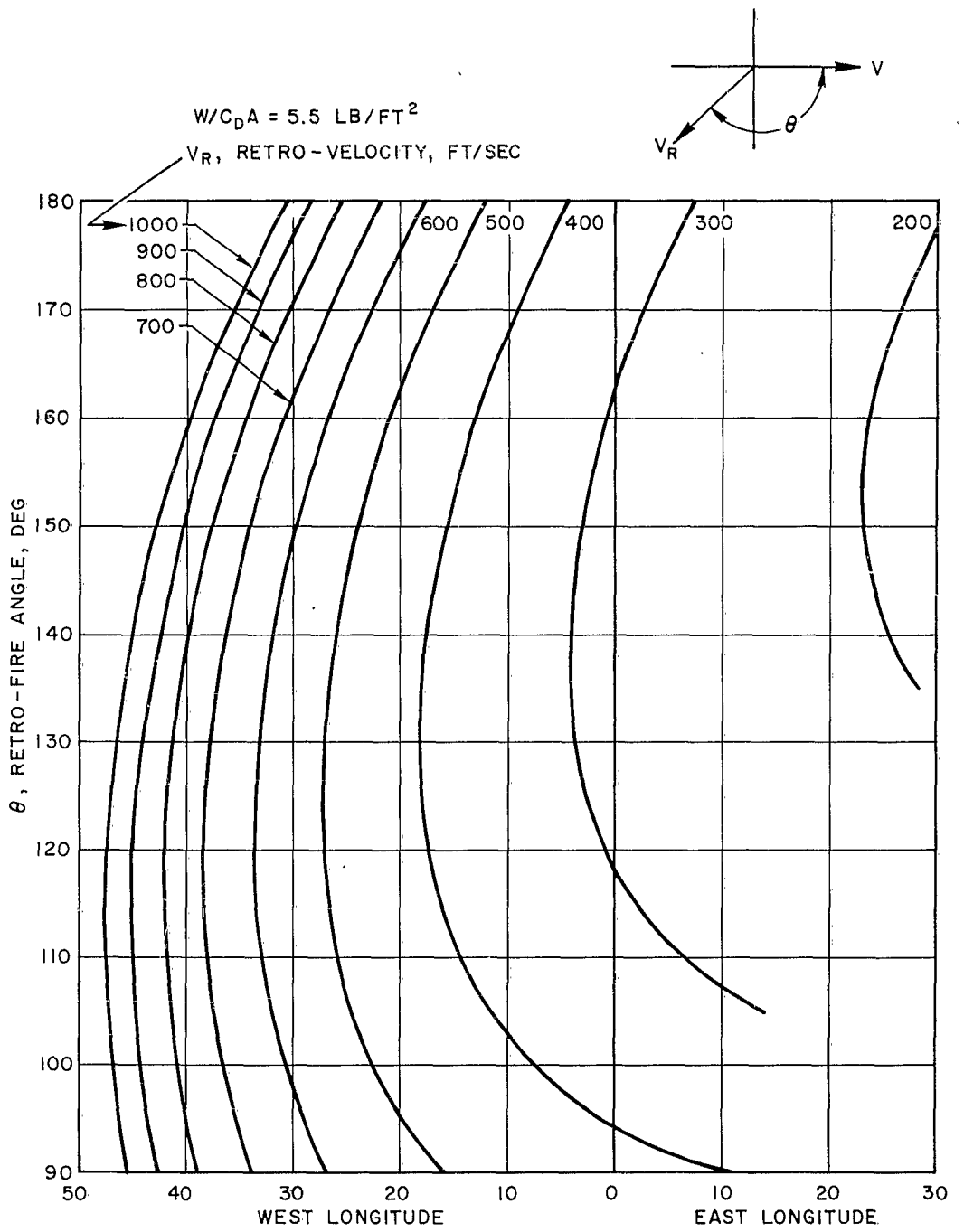


Figure 5. Impact Longitude as a Function of Retro-fire Angle and Retro-velocity.

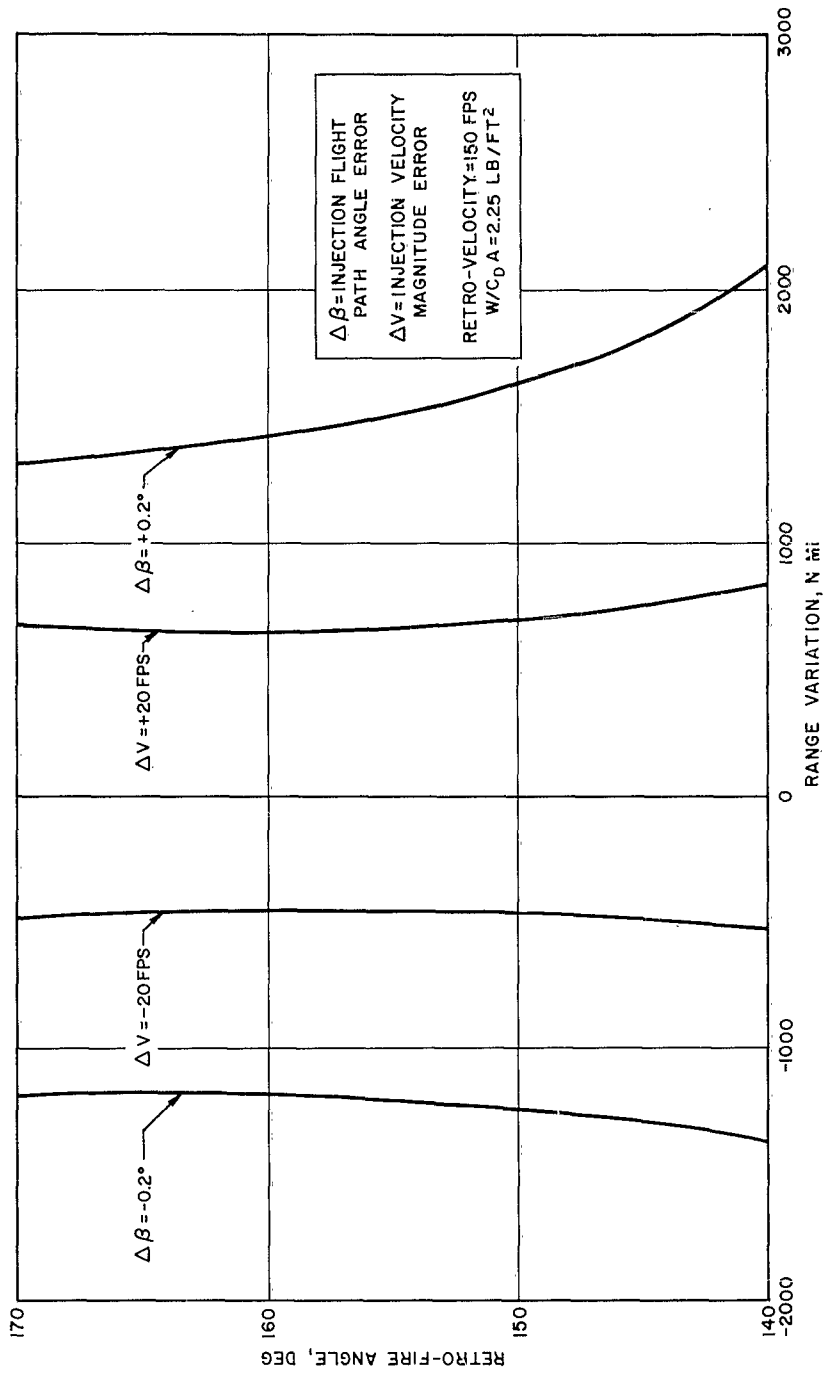


Figure 6. Impact Range Variation as a Function of Injection Errors and Retro-fire Angle  
 Retro-velocity = 150 fps,  $W/C_{DA} = 2.25 \text{ lb/ft}^2$ .

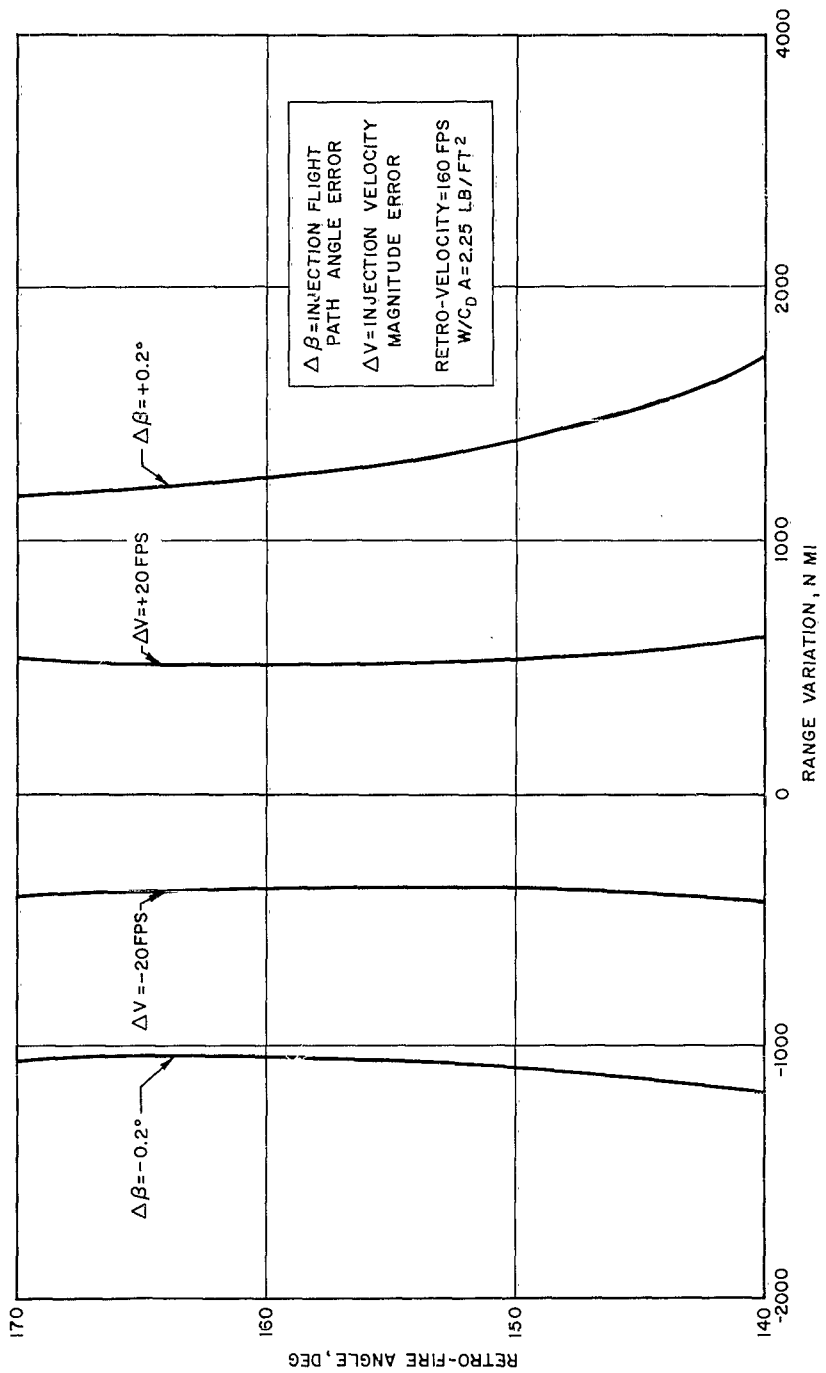


Figure 7. Impact Range Variation as a Function of Injection Errors and Retro-fire Angle.  
 Retro-velocity = 160 fps,  $W/C_{DA} = 2.25 \text{ lb/ft}^2$ .

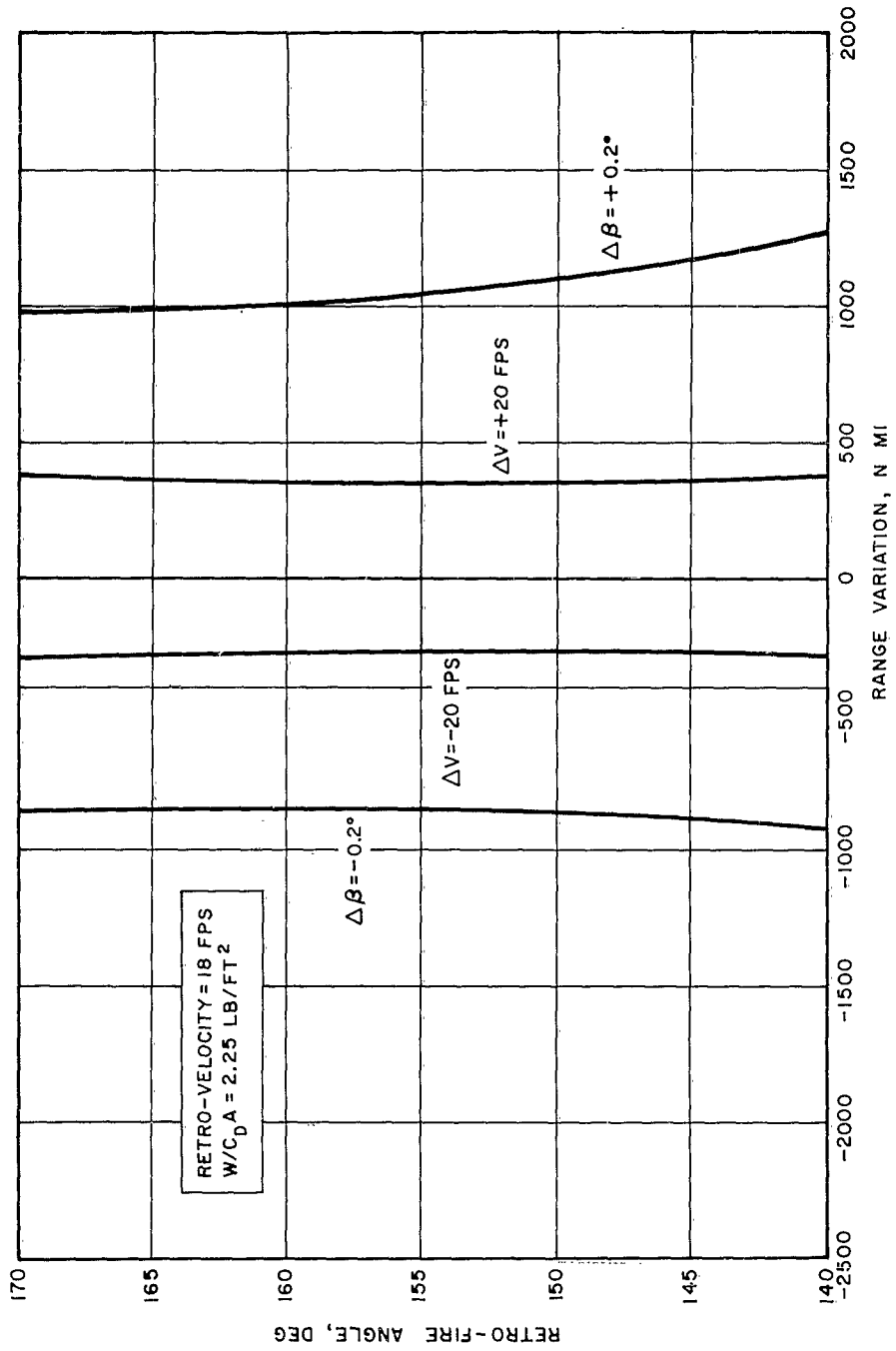


Figure 8. Impact Range Variation as a Function of Injection Errors and Retro-fire Angle.  
Retro-velocity = 18 fps,  $W/C_{DA} = 2.25 \text{ lb/ft}^2$ .

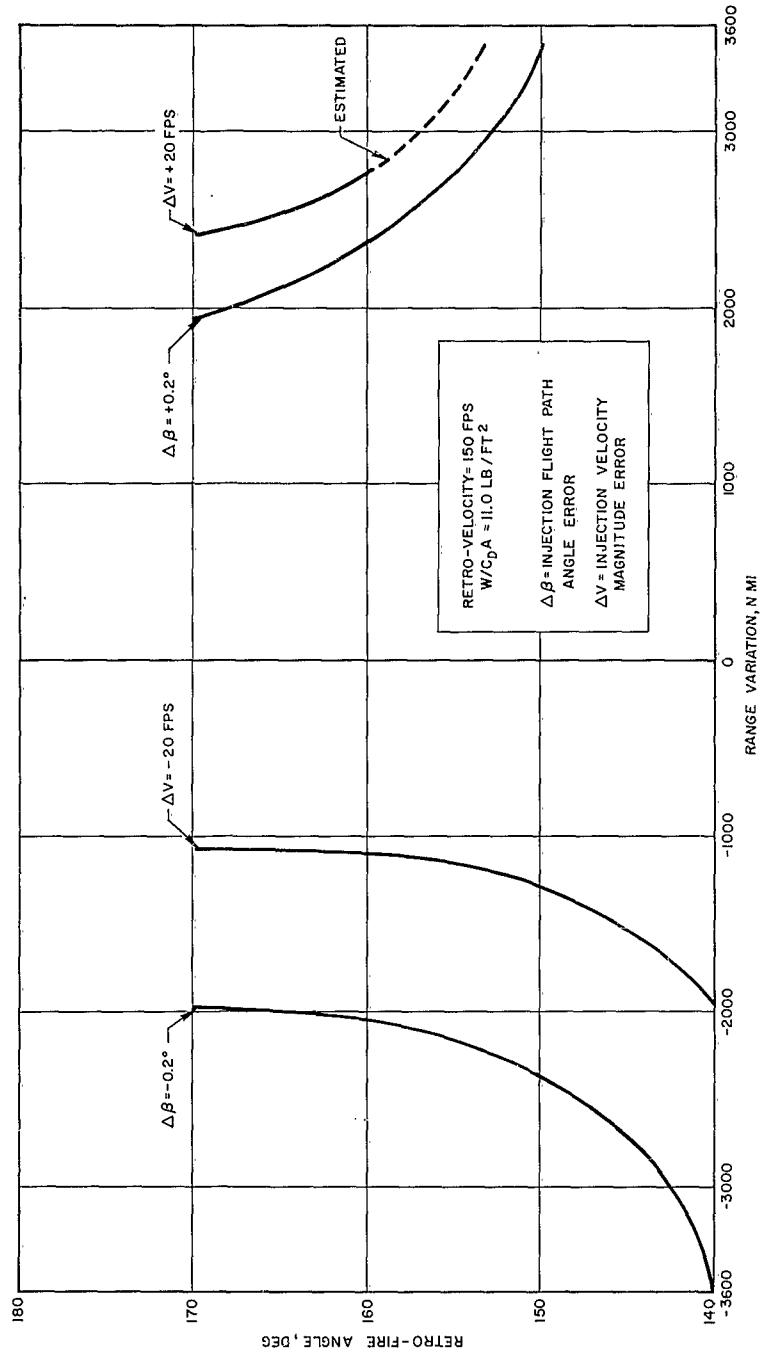


Figure 9. Impact Range Variation as a Function of Injection Errors and Retro-fire Angle.  
 Retro-velocity = 150 fps,  $W/C_{DA} = 11.0 \text{ lb/ft}^2$ .

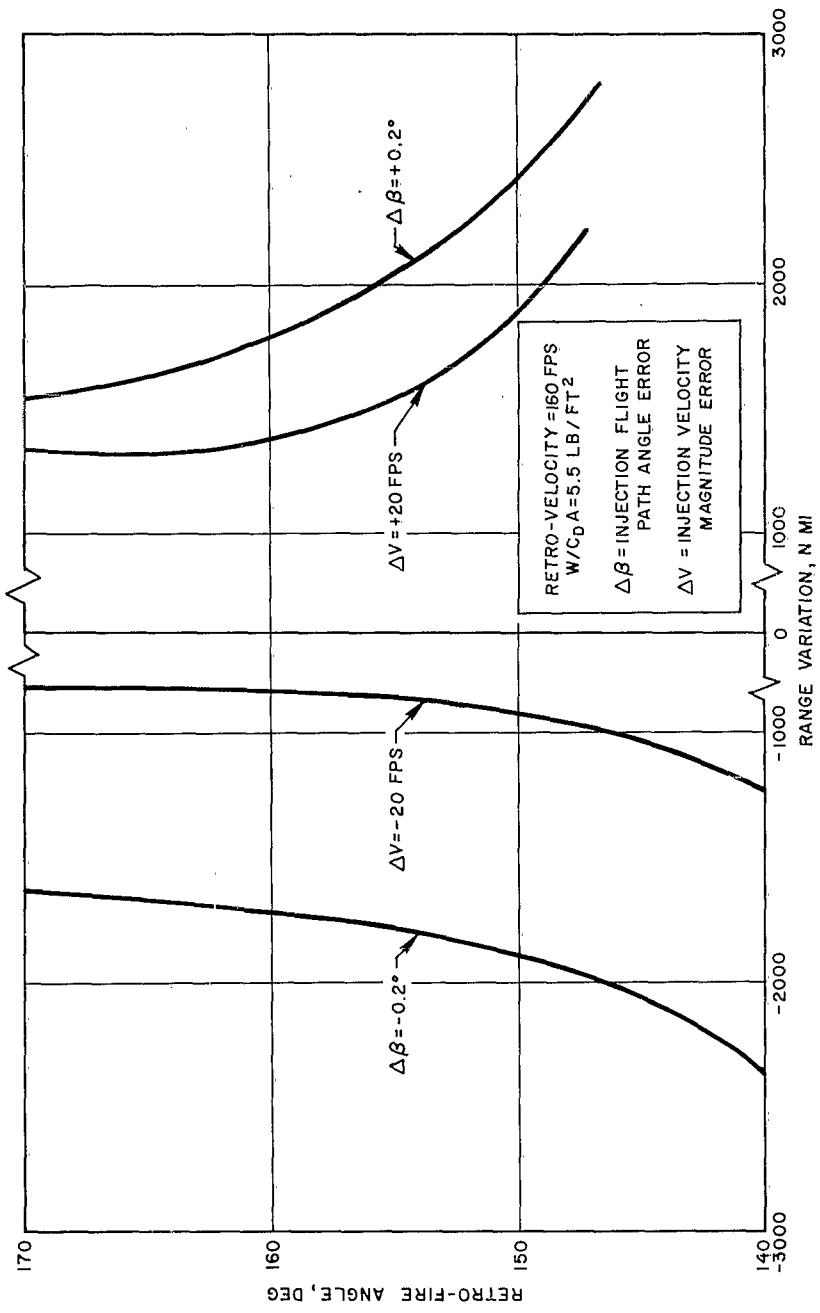


Figure 10. Impact Range Variation as a Function of Injection Errors and Retro-fire Angle.  
 Retro-velocity = 160 fps,  $W/C_{D A} = 5.5 \text{ lb/ft}^2$ .

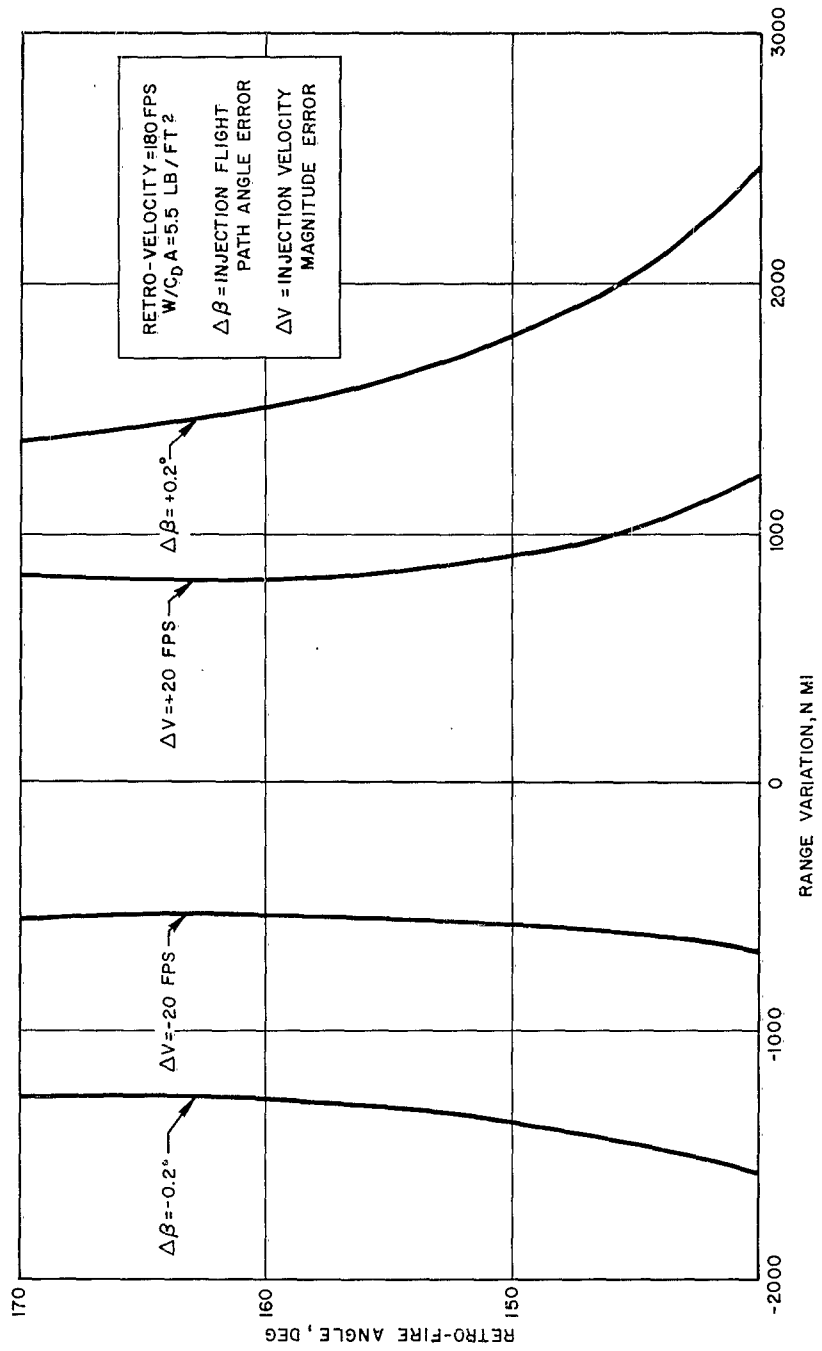


Figure 11. Impact Range Variation as a Function of Injection Errors and Retro-fire Angle.  
 Retro-velocity = 180 fps,  $W/C_{DA} = 5.5 \text{ lb/ft}^2$ .

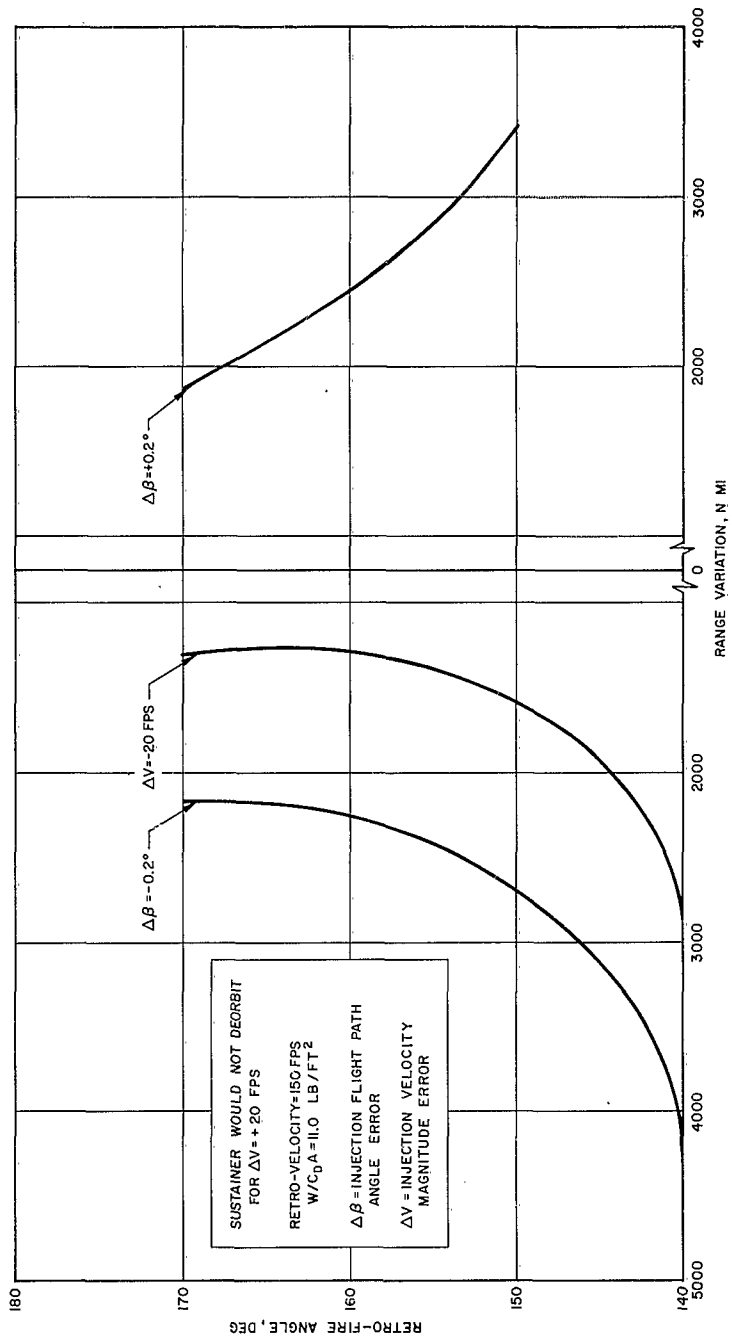


Figure 12. Impact Range Variation as a Function of Injection Errors and Retro-fire Angle.  
 Retro-velocity = 150 fps,  $W/C_{DA} = 11.0$  lb/ft<sup>2</sup>.

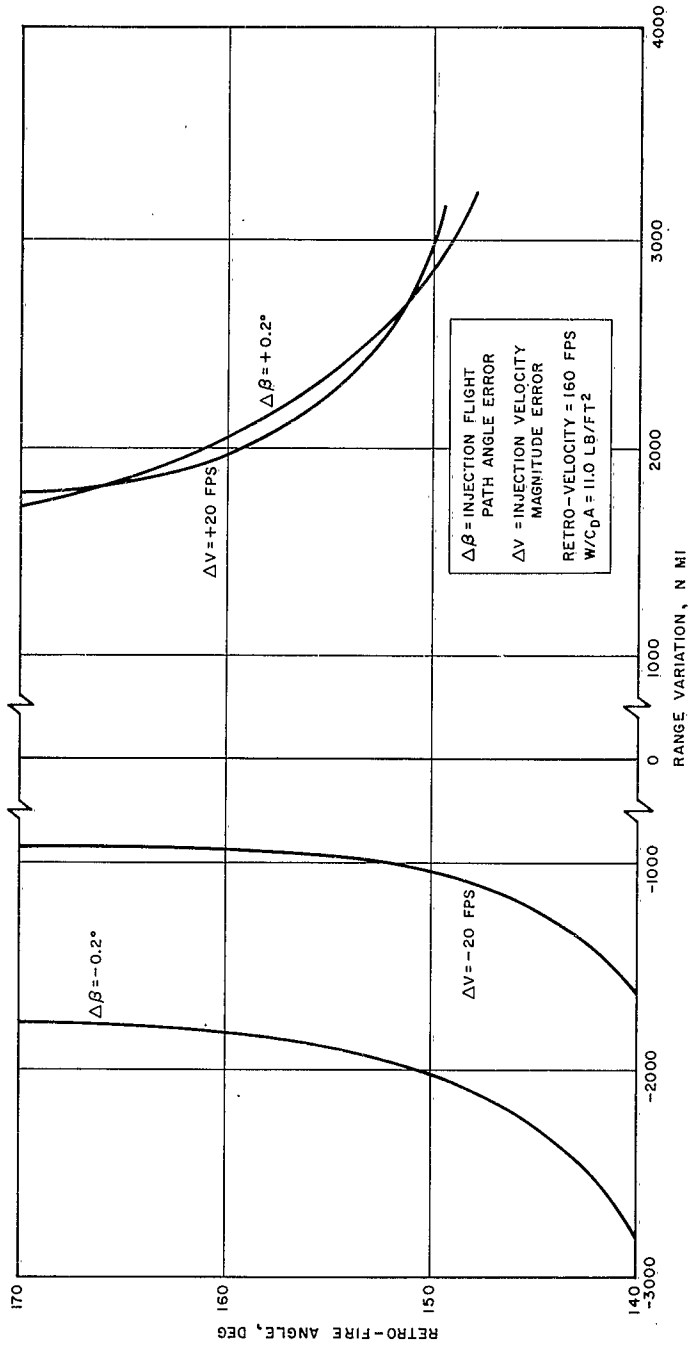


Figure 13. Impact Range Variation as a Function of Injection Errors and Retro-fire Angle. Retro-velocity = 160 fps,  $W/C_{DA} = 11.0 \text{ lb/ft}^2$ .

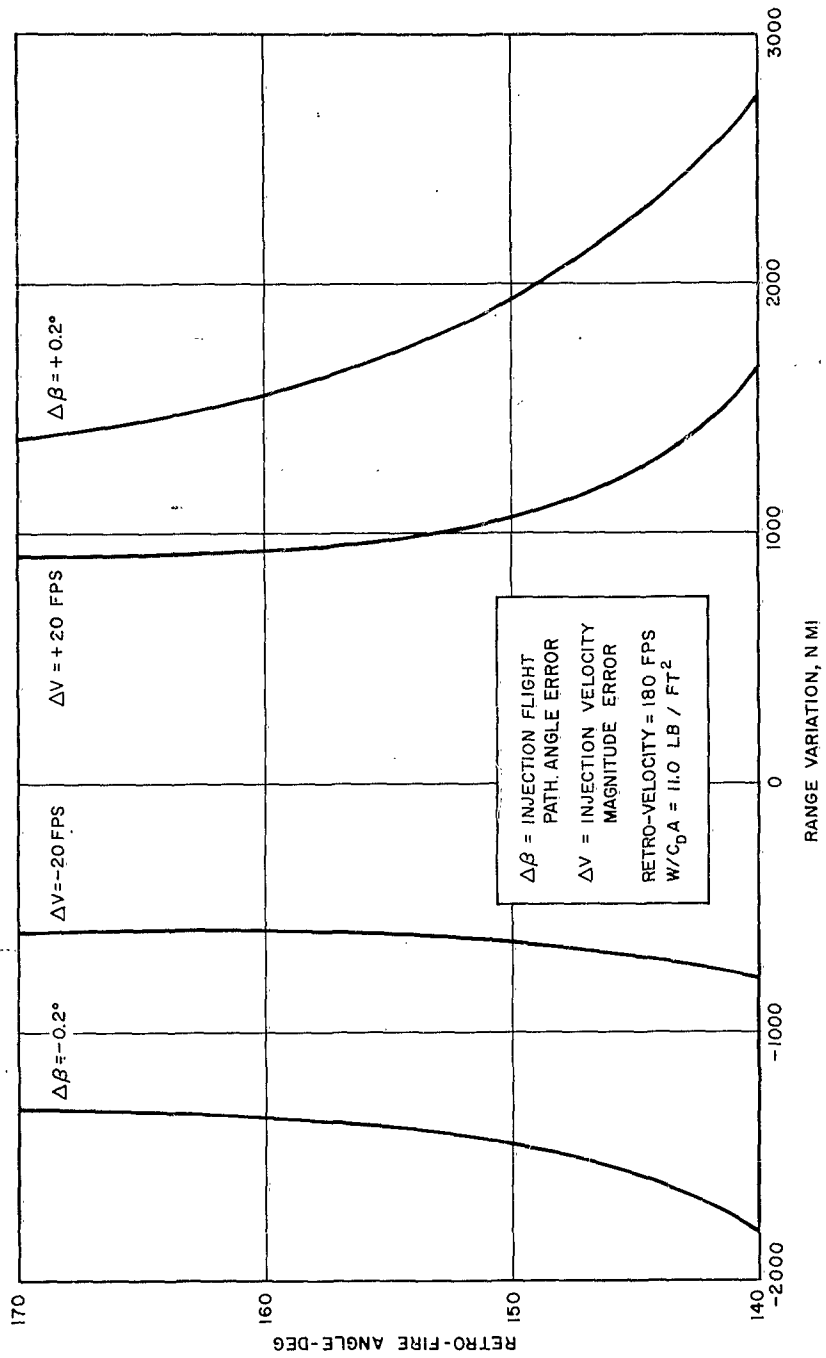


Figure 14. Impact Range Variation as a Function of Injection Errors and Retro-fire Angle.  
 Retro-velocity = 180 fps,  $W/C_{DA} = 11.0$  lb/ft<sup>2</sup>

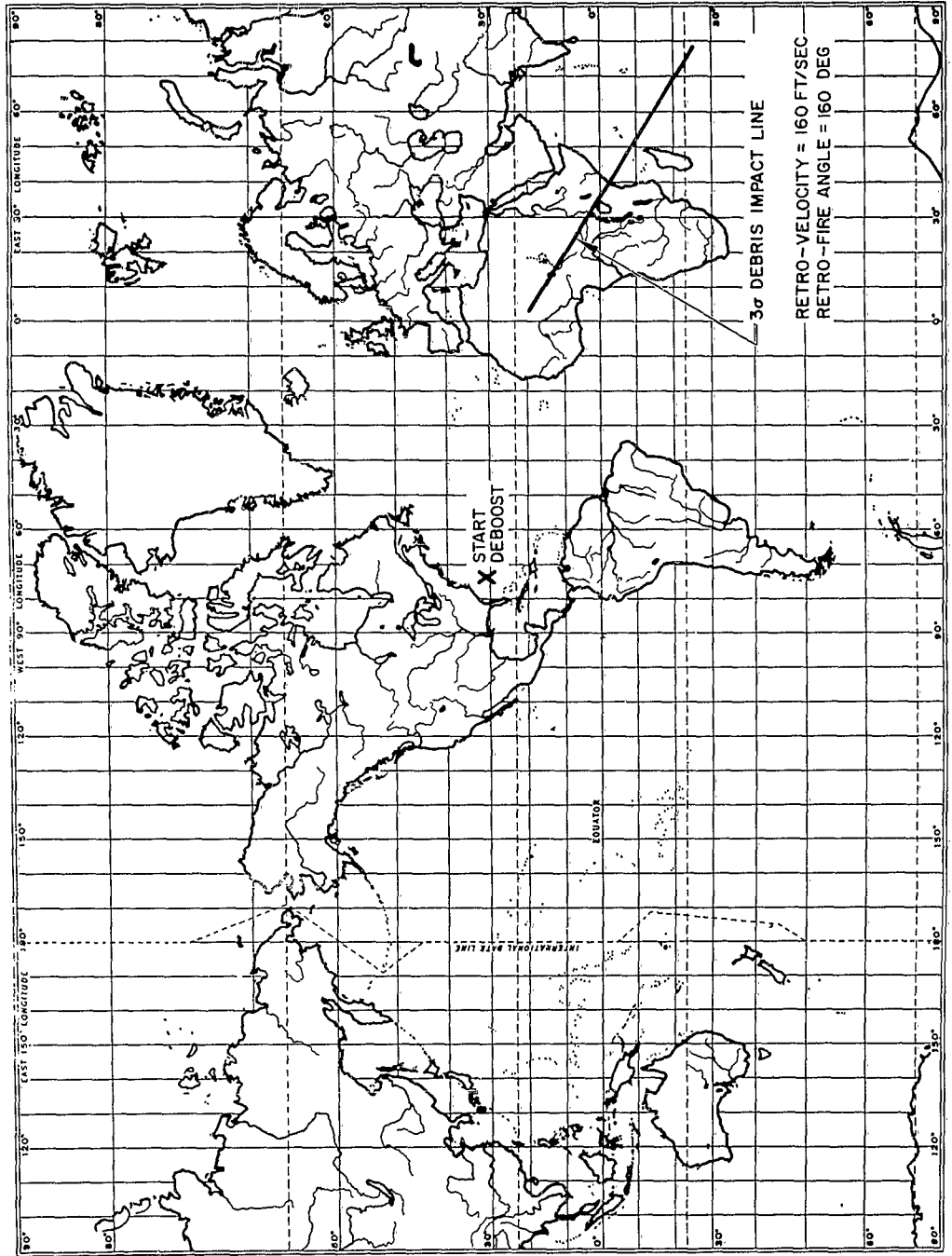


Figure 15. Expected Debris Impact Line from  $\pm$  Three Sigma Injection Flight Path Angle Errors.

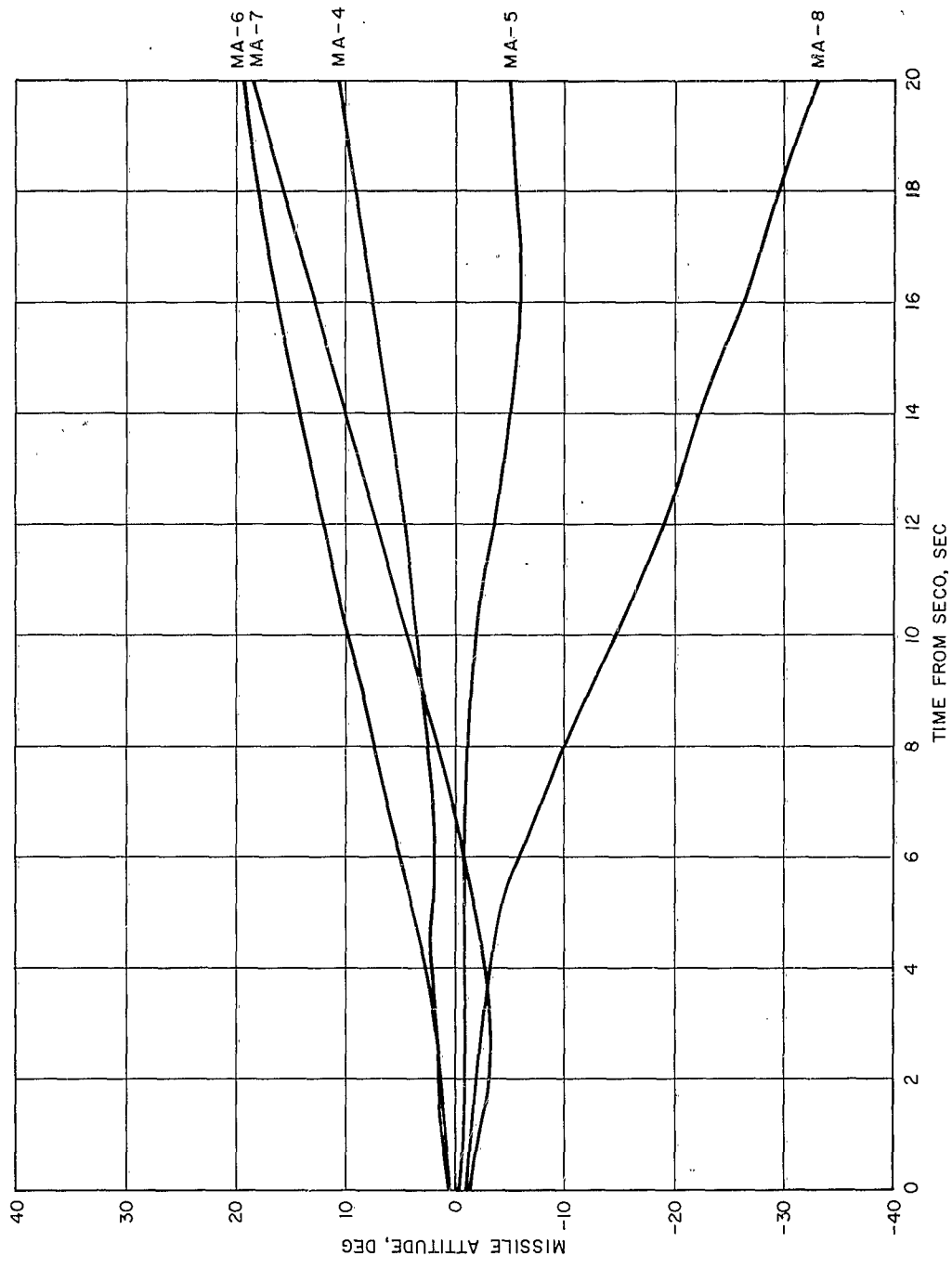


Figure 16. Missile Pitch Attitude versus Time from SECO to SECO + 20 sec.

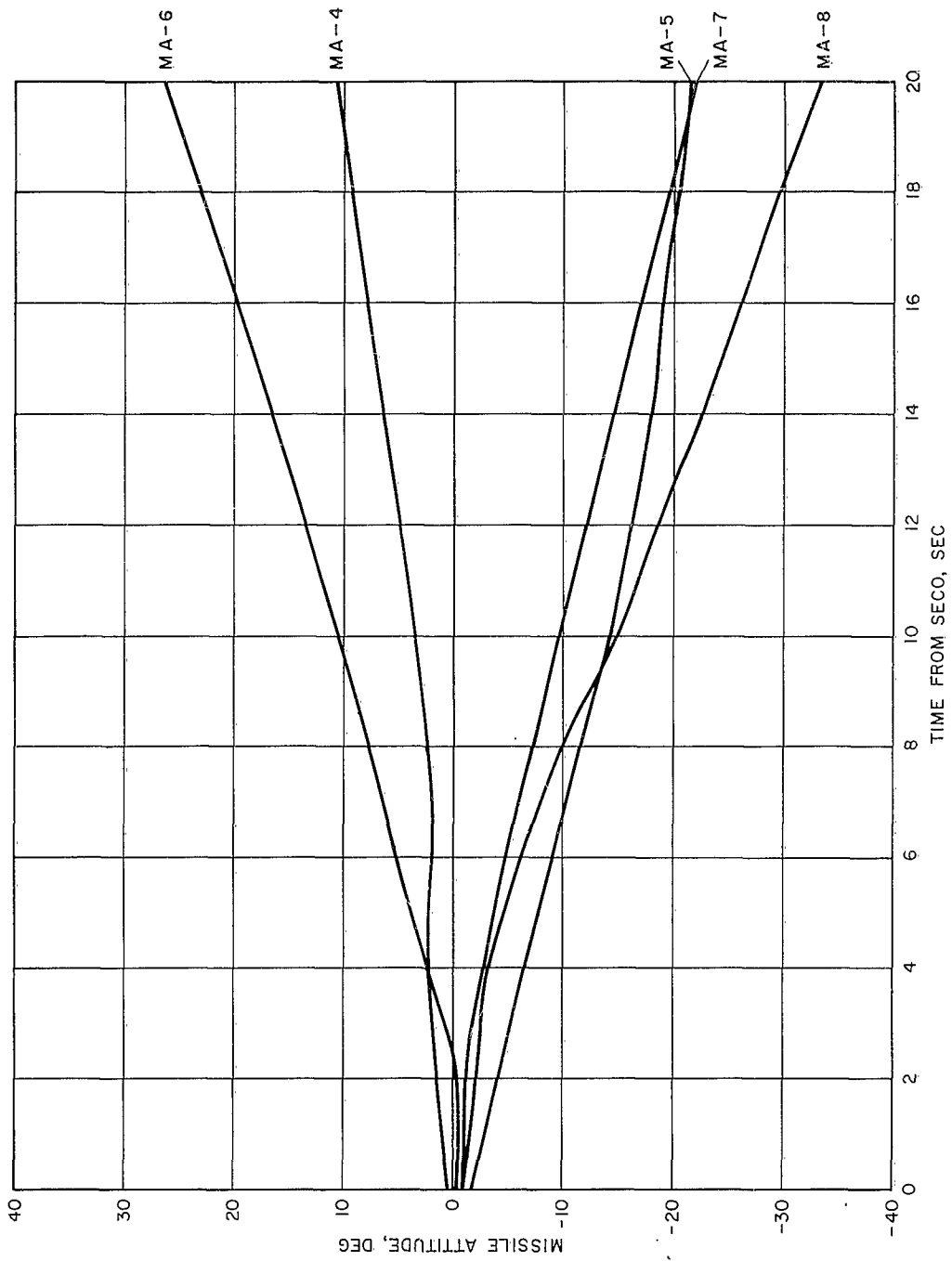


Figure 17. Missile Yaw Attitude versus Time from SECO to SECO + 20 sec.

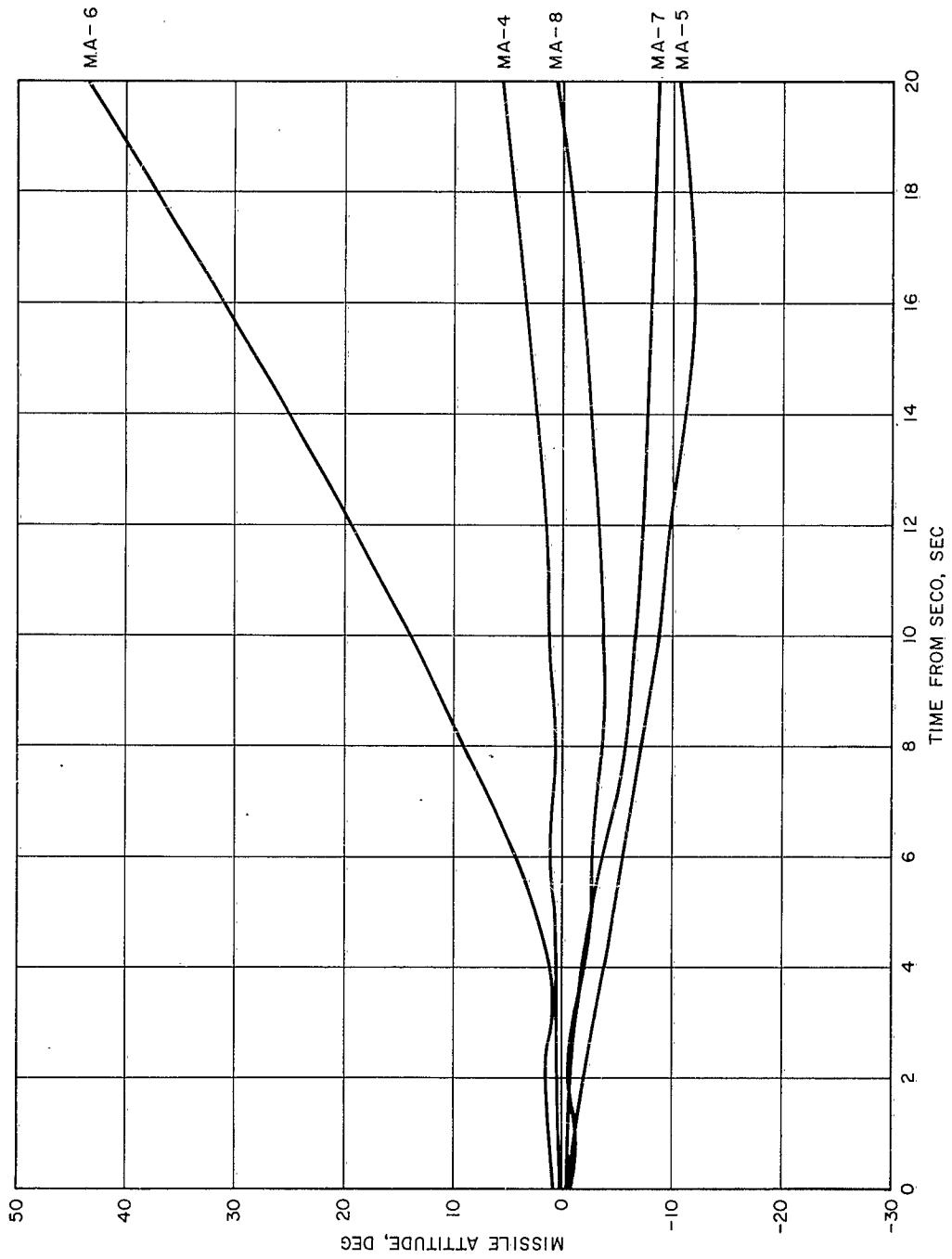


Figure 18. Missile Roll Attitude versus Time from SECO to SECO + 20 sec.

UNCLASSIFIED	<p>Aerospace Corporation, El Segundo, California. FEASIBILITY STUDY OF THE CONTROL OF THE MERCURY/ATLAS BOOSTER RE-ENTRY FROM ORBITAL MISSIONS, prepared by D. Pace and T. Shiohara. 15 May 1963. [58]p. incl. illus. (Report TDR-169(3101)TN-1; SSD-TDR-63-106) (Contract AF 04(695)-169) Unclassified report</p> <p>An investigation was undertaken into the feasibility of deorbiting the Mercury/Atlas booster in such a way as to prevent fragments of the booster from falling on land masses and to do this without compromising Mercury mission objectives. This report summarizes the various methods explored and presents the conclusions thereof.</p>	UNCLASSIFIED
--------------	---	--------------

UNCLASSIFIED	<p>Aerospace Corporation, El Segundo, California. FEASIBILITY STUDY OF THE CONTROL OF THE MERCURY/ATLAS BOOSTER RE-ENTRY FROM ORBITAL MISSIONS, prepared by D. Pace and T. Shiohara. 15 May 1963. [58]p. incl. illus. (Report TDR-169(3101)TN-1; SSD-TDR-63-106) (Contract AF 04(695)-169) Unclassified report</p> <p>An investigation was undertaken into the feasibility of deorbiting the Mercury/Atlas booster in such a way as to prevent fragments of the booster from falling on land masses and to do this without compromising Mercury mission objectives. This report summarizes the various methods explored and presents the conclusions thereof.</p>	UNCLASSIFIED
--------------	---	--------------

UNCLASSIFIED	<p>Aerospace Corporation, El Segundo, California. FEASIBILITY STUDY OF THE CONTROL OF THE MERCURY/ATLAS BOOSTER RE-ENTRY FROM ORBITAL MISSIONS, prepared by D. Pace and T. Shiohara. 15 May 1963. [58]p. incl. illus. (Report TDR-169(3101)TN-1; SSD-TDR-63-106) (Contract AF 04(695)-169) Unclassified report</p> <p>An investigation was undertaken into the feasibility of deorbiting the Mercury/Atlas booster in such a way as to prevent fragments of the booster from falling on land masses and to do this without compromising Mercury mission objectives. This report summarizes the various methods explored and presents the conclusions thereof.</p>	UNCLASSIFIED
--------------	---	--------------

UNCLASSIFIED	<p>Aerospace Corporation, El Segundo, California. FEASIBILITY STUDY OF THE CONTROL OF THE MERCURY/ATLAS BOOSTER RE-ENTRY FROM ORBITAL MISSIONS, prepared by D. Pace and T. Shiohara. 15 May 1963. [58]p. incl. illus. (Report TDR-169(3101)TN-1; SSD-TDR-63-106) (Contract AF 04(695)-169) Unclassified report</p> <p>An investigation was undertaken into the feasibility of deorbiting the Mercury/Atlas booster in such a way as to prevent fragments of the booster from falling on land masses and to do this without compromising Mercury mission objectives. This report summarizes the various methods explored and presents the conclusions thereof.</p>	UNCLASSIFIED
--------------	---	--------------